PARAMETRIC ANALYSIS OF AIR TO AIR TUBULAR CROSS FLOW HEAT EXCHANGER USING COMPUTATIONAL FLUID DYNAMICS

A
Thesis

submitted in partial fulfillment of the requirements for the award of degree of

Master of Engineering (M.E.)

In
Thermal Engineering

Submitted by
LAKSHYA GARG
(ROLL NO. 801383016)

UNDER THEGUIDANCE OF

Mr. Sumeet Sharma
Associate Professor
(MED)

Dr. D. Gangacharyulu
Professor
(CHED)

DEPARTMENT OF MECHANICAL ENGINEERING
THAPAR UNIVERSITY, PATIALA – 147004
JULY 2015

CERTIFICATION

I, Lakshya Garg, declare that this thesis report entitled "***Parametric Analysis of air to air tubular cross flow heat exchanger using computational fluid dynamics***", submitted towards fulfillment of the requirements for the award of Master's Degree in Thermal Engineering, in Mechanical Engineering Department of Thapar University, Patiala, is entirely my own work. This document has not been submitted for any degree in any other institution.

Lakshya Garg

Date: 15/07/2015

Place: PATIALA

Lakshya Garg

801383016

Thapar University, Patiala

This is to certify that above statement made by the candidate is correct and true to the best of my knowledge.

Mr. Sumeet Sharma
Associate Professor
(MED)

Dr. D Gangacharyulu
Professor
(CHED)

Countersigned by

Dr. S.K. Mohapatra
Sr. Professor and Head
Mechanical Engineering Department
Thapar University, Patiala

Dr. S.S. Bhatia
Dean
Academic Affairs
Thapar University, Patiala

ACKNOWLEDGEMENT

I would like to express my deepest gratitude to my supervisors, Mr. Sumeet Sharma and Dr. D. Gangacharyulu, for their excellent guidance, caring, patience, and providing me with an excellent atmosphere for doing research. Your advice on both research as well as on my career have been priceless. The opportunity, support, exposure and atmosphere provided by the Thapar University, Patiala, to carry out my studies are highly appreciated.

A special debt of gratitude is owed to the authors whose works I have consulted and quoted in this work. Last but not least, I am forever grateful to my parents, family and friends for their unconditional support and best wishes.

Lakshya Garg

801383016

ABSTRACT

Air to air tubular cross flow heat exchanger used for cooling of large electric motors has been taken for study. The computational fluid dynamics analysis was done by using ANSYS FLUENT 15.0 on heat exchanger and obtained results were compared with experimental results. Then, the actual model was simulated by varying the cold air inlet velocities from 14 to 20 m/s using CFD. A computer program was developed using MATLAB programming based on analytical formulation of heat exchanger using ε-NTU technique for actual design. The results obtained from the MATLAB program at different velocities has shown close agreement with the CFD simulation results. Two models were also modelled by changing the geometrical parameters such as baffle position and number of tubes. Simulation was performed and results were compared with the actual model. It has been seen that there is not much change in temperature distribution of hot and cold air on shifting of baffle locations. It is found that with increase in cold air inlet velocities, there is not significant change in outlet temperatures of both hot and cold air, whereas pressure drop has shown parabolic increasing trend. Also, on addition of three additional tubes the values of temperatures of hot and cold air has decreased, so an optimum model with three additional cold air tubes and 14 m/s cold air inlet velocity was proposed and it was seen that the thermal performance of heat exchanger has increased even with lower cold air flow rates and pressure drops.

TABLE OF CONTENTS

LIST OF FIGURES

LIST OF TABLES

Page No.

Nomenclature

A_1: Transverse Plane

A_2: Diagonal Plane

A_c: Cross-sectional Area [m^2]

C_1: Constant

C_2: Constant

D: Tube Diameter [m]

D_h: Hydraulic Diameter [m]

L: Length of Tube [m]

L_h: Hydrodynamic Entry Length [m]

L_t: Thermal Entry Length [m]

N_L: Number of rows

Nu: Average Nusselt Number

Pr: Prandtl Number

Pr_s: Prandtl Number corresponding to Surface Temperature

Re: Reynold Number

S_D: Diameteral Pitch [m]

S_T: Transverse Pitch [m]

T_b: Bulk Mean Temperature [K]

T_e: Average Temperature at exit of Pipe [K]

T_i: Average Temperature at entry of Pipe [K]

V: Volume Flow Rate [m^3/s]

V_{max}: Maximum Fluid Velocity [m/s]

f: Friction Factor

h: Average Convective Heat Transfer Coefficient [W/m^2K]

k: Thermal Conductivity [W/mK]

m: Constant

n: Constant

p: Perimeter of Tube [m]

v: Velocity of Fluid [m/s]

ρ: Density of Fluid [kg/m^3]

μ_b: Dynamic Viscosity of Fluid at Bulk Mean Temperature [Pa s]

μ_s: Dynamic viscosity of Fluid at Surface Temperature [Pa s]

Δp: Pressure Drop [Pa]

χ: Correction Factor

CHAPTER 1: INTRODUCTION AND OBJECTIVES

1.1 Introduction

Cross flow heat exchangers are widely used in thermal systems. Based on construction, cross flow heat exchanger are two types: Tube with fins and tubes heat without fins. Fins are used with cross flow heat exchangers when there is huge difference between the heat transfer coefficients of hot and cold mediums, such as water and air. In such cases, fins are required to increase the heat transfer area along the air side to augment the heat transfer rate, but at the expense of power requirement; because finned type heat exchangers have more pressure drop as compared to without fin heat exchangers (Toolthaisong and Kasayapanand, 2013). Hence, fin is not a necessary installation in case of heat exchangers, when the heat transfer is occurring between the mediums having almost same heat transfer coefficients. There are also several other arrangements to increase the rate of heat transfer such as shape and arrangement tubes, position of baffles etc. According to Gomez et al., 2009, the thermal effectiveness of a cross flow heat exchanger could be upgraded by a more uniform temperature difference field. This can be attained in two different ways: either redistributing the heat transfer area or rearranging the connections between tubes. Different methods have been adopted by Chang et at., 2010, which aims at enhancing the fan performance by changing the geometry, redesigning new heat exchanger with guide vanes and optimizing the distance between axial fans.

Cross flow heat exchangers have a wide range of applications such as in air pre-heater, economiser, super-heater in thermal power plants, automotive radiator and cooling of large electrical motors, etc (Ishak et al., 2013). Air to air tubular cross flow heat exchangers are

used for cooling of large electric motors in various industries. There is generation of enormous amount of heat due to energy loses in the windings of electrical motors at various loads. So, air is circulated across motor windings is cooled by using air to air tubular cross flow heat exchanger. These types of heat exchangers require low operational as well as maintenance cost due to use of air and simple tubes.

Although, the electric motors are the critical component of all the industrial systems (Gomez et al., 2009), but yet very little work has been carried to improve the cooling of electric motors. The improper cooling of motors leads to overheating, which leads to decrease in the performance of motors and sometimes may damage the windings of motors. Hence, the effort should be made to reduce the temperature of motors by providing effective cooling techniques. Therefore, the further research is needed to improve design an effective heat exchanger that would enhance the cooling rate and result in lower temperatures across windings of electric motors. Hence, the present study has been carried out to study the pressure, temperature and velocity distribution of hot and cold air in tubular cross flow heat exchanger using commercial code, Fluent. A MATLAB program was also developed for the actual model and results were validated with CFD results. Air to air cross flow tubular heat exchanger has been taken for simulation using Computational Fluid Dynamics (Kumar et al., 2003).

1.2 Objectives

In the context of above limitations the following specific objectives have been undertaken in the present study:

1. To simulate the air to air tubular cross flow heat exchangers by using CFD and to obtain temperature as well as pressure distributions for same.

2. To perform the simulation by changing the geometrical and flow parameters of heat exchanger to maximize the heat transfer rates.

3. Develop a model using MATLAB programming to design similar type of heat exchanger with similar type of mission for varying capacity.

CHAPTER 2: LITERATURE REVIEW

2.1 Heat exchangers

The devices which are used to exchange heat energy from one medium to another, called heat exchangers. Mediums may or may not be in direct contact with each other. The fluid having lower thermal energy gains heat from the fluid having higher thermal energy. So, heat exchangers serve the purpose of both heating and cooling in industrial and domestic thermal systems. Different types of heat exchangers are available according to their application. Common areas of heat exchanger applications are space heating, air conditioning, chemical industries, power plants etc. One of the examples of compact cross flow heat exchanger is radiator of automobile engine.

The advantages of air to air heat exchangers are:

1. As air is used as cooling medium so disadvantages related to water cooled heat exchangers are eliminated like expense of treating water, chemical pollution of water resources, pumping of water, elimination of water fouling, independent of source of water location, frequent cleaning, loss of water due to evaporation, etc.
2. Very less power requirement is needed for operation of air to air heat exchangers.
3. No vibrational problems.
4. No problems due to corrosion, algae, scale etc. due to water cooling
5. Air to air heat exchangers can work even through power failure due to radiation and natural convection.

6. Maintenance is generally lower compared to water cooling systems. Tubes and fins can be cleaned by compressed air and brushes even while in operation.

Limitations of air to air heat exchangers are:

1. Air has relatively poor thermal transport properties when compared to water. As a result, heat transfer area of air to air heat exchangers is more as compared to water cooled heat exchangers for same capacity.
2. Noise due to air turbulence and high fan tip speed is generated. This is due to movement of large volumes of cooling air accomplished by rotation of large diameters of fan blades rotating at high speed.
3. Capital costs of air to air heat exchangers are high when compared to water cooled heat exchangers on same heat load.
4. Pressure leakages are also more in case of air to air heat exchangers under vacuum.

2.2 Classification of heat exchangers

Heat exchangers are mainly used in power plants, automobiles, air conditioning, HVAC systems petroleum refineries, heat recovery systems, manufacturing plants etc. Heat exchangers can be classified into numerous ways. Common basis of classification are heat transfer methods, number of fluids and transfer processes. Heat exchangers are further classified according to flow arrangements and construction type. They can also be classified based on the heat transfer surface area/volume ratio, into compact and non compact heat exchangers.

Based on flow:

- *Parallel flow:* both the hot and cold fluids enter the heat exchanger at the same end and move in the same direction.
- *Counter flow:* the hot and cold fluids enter the heat exchanger at opposite ends and flow in opposite directions.
- *Cross flow:* the flow of hot and cold fluids is perpendicular to each other.

Based on construction:

Based on construction heat exchangers are classified in many ways. The simplest type of heat exchanger consists of two concentric pipes of different diameters, called the double-pipe heat exchanger. One fluid in a double-pipe heat exchanger flows through the smaller pipe while the other fluid flows through the annular space between the two pipes.

Another common configuration is shell and tube heat exchanger. Specific forms differ according to the number of shell and tube passes, simplest form of this type involves the single shell and tube pass. Baffles are generally installed to increase the shell side convective heat transfer coefficient by inducing turbulence and cross flow velocity component. In addition, baffles also support the tubes physically and reduce the flow induced tube vibrations. Another type of heat exchanger, which is specifically designed to realize a large heat transfer surface area per unit volume, is the compact heat exchanger. The ratio of the heat transfer surface area of a heat exchanger to its volume is called the area density. A heat exchanger with area density greater than 700 m^2/m^3 is classified as being compact. Examples of compact heat exchangers are car radiators (1000 m^2/m^3) and the human lung (20,000 m^2/m^3).

Cross Flow Heat Exchangers:

In cross flow heat exchangers, the two fluids usually move perpendicular to each other, and such flow configuration is called cross-flow. The cross flow tubular heat exchangers may be finned and unfinned tubular heat exchangers as shown in following figure.

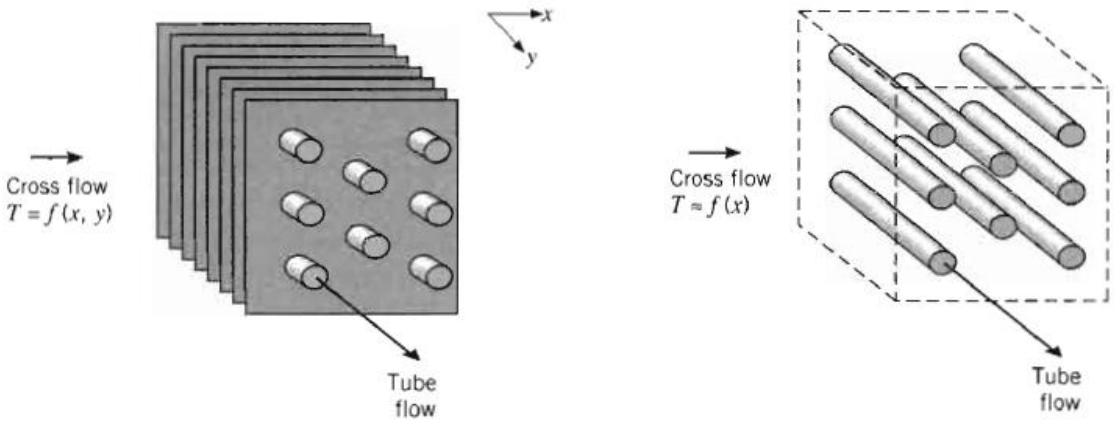

Figure 2.1: Finned and unfinned tubular heat exchanger (Incropera and Dewitt, 2002)

In finned tubular heat exchanger the fluid is said to be unmixed because the fin inhibits the motion of fluid in a direction that is transverse to the main flow direction. In this case the temperature of the fluid varies in both directions whereas for unfinned tube bundles the mixing is possible in tranverse directions hence the temperature variations are primarily in main flow direction. The nature of mixing condition can significantly influence heat exchanger performance.

Cross-flow recuperators are compact tubular air-to-air heat exchangers designed to recover the waste heat in industrial exhaust gases. The recovered heat is used to preheat the combustion air for the system's burners, thereby increasing the thermal efficiency.

Electric motors are used most widely for the industrial applications. The significant amount of heat generates in the windings of thee electric motors due to the energy losses. For the efficient operation of the motors this heat must be removed so cold air is blown through windings of the motors that carries the heat generated and as a result it becomes hot when

comes out of the motor casing. Now this hot air is cooled by passing it across the tube bundles inside which cold air is flowing. Since across the tube bundles both the fluids are air so this configuration is called as air to air heat exchanger. Tubes are arranged in the manner so that the flow of hot air across the tubes should be perpendicular to the direction of flow of cold air stream. So the term cross flow is used. Hence the aim of this study is to analyze, design and to optimize air to air tubular cross flow heat exchanger for cooling of electric motors.

2.3 Design of cross flow tubular heat exchangers

To calculate the required area of heat transfer for a heat exchanger, the overall heat transfer coefficient must be determined and for calculating the overall heat transfer coefficient, the convective heat transfer coefficient inside and outside the tube must be known. As the fluid flows through or across the tubes the pressure drop takes place. This pressure drop must be determined in order to calculate the power requirement of blower or compressor. For the air to air tubular heat exchangers the problem is divided into two major categories. For the air flow inside the tubes, the relations of forced internal convective heat transfer will be applicable and for flow across the tubes, external forced convection relation will be applicable.

2.4 Analysis of flow through tubes

Flow through tubes can be classified into two flow regions: laminar and turbulent flow. Reynolds number based criteria was used to decides whether the flow is laminar or turbulent. These flows are further classified into hydro-dynamically and thermally developing or fully developed flows. There are various correlations available based on the nature of flow for Nusselt number and pressure drop. Some of the correlations are mentioned below.

Nusselt number for the thermal entrance region can be determined from Edwards et al., (1979):

$$Nu = 3.66 + \frac{\left[0.065\left(\frac{D}{L}\right)RePr\right]}{\left[1 + 0.04\left\{\left(\frac{D}{L}\right)RePr\right\}\right]^{\frac{2}{3}}}$$

This relation assumes that the flow is hydro-dynamically developed when the fluid enters the heating section, but it can also be used approximately for hydro-dynamically developing flows. When the difference between the surface and the fluid temperatures is large, it may be necessary to account for the variation of viscosity with temperature. The average Nusselt number for developing laminar flow in a circular tube in that case can be determined from Sieder and Tate (1936):

$$Nu = 1.86\left(RePr\ \frac{D}{L}\right)^{1/3}\left(\frac{\mu_b}{\mu_s}\right)^{0.14}$$

All properties are evaluated at the bulk mean fluid temperature, except for μ_s, which is evaluated at the surface temperature. The Nusselt number in turbulent flow is related to the friction factor through the Chilton–Colburn analogy expressed as:

$$Nu = 0.125f\ RePr^{1/3}$$

Once the friction factor is available, this equation can be used conveniently to evaluate the Nusselt number for both smooth and rough tubes. For fully developed turbulent flow in smooth tubes, a simple relation for the Nusselt number can be obtained by substituting the simple power law relation $f = 0.184\ Re^{-0.2}$. It gives:

$$Nu = 0.023\ Re^{0.8}\ Pr^{1/3}$$

This is known as the Colburn equation. The accuracy of this equation can be improved by modifying it as:

$$Nu = 0.023\ Re^{0.8}\ Pr^{n}$$

Where n = 0.4 for heating and n = 0.3 for cooling of the fluid flowing through the tube. This equation is known as the Dittus-Boelter equation and it is preferred to the Colburn equation. The fluid properties are evaluated at the bulk mean fluid temperature $T_b = (T_i - T_e)/2$. When the temperature difference between the fluid and the wall is very large, it may be necessary to use a correction factor to account for the different viscosities near the wall and at the tube center. The Nusselt number relations above are fairly simple, but they may give errors as large as 25 percent. This error can be reduced considerably to less than 10 percent by using more complex but accurate relations such as the second Petukhov equation expressed as:

$$Nu = \frac{\left(\frac{f}{8}\right) RePr}{1.07 + 12.7\left(\frac{f}{8}\right)^{0.5}(Pr^{2/3} - 1)} \qquad \begin{pmatrix} 0.5 \le Pr \le 2000 \\ 10^4 < Re < 5 * 10^6 \end{pmatrix}$$

2.5 Flow across tubes

Heat transfer to or from a bank of tubes in cross flow is relevant to numerous industrial applications, such as steam generation in a boiler or air cooling in the coil of an air conditioner. The tube rows of a bank are either staggered or aligned in the direction of fluid velocity. The configuration is characterized by tube diameter d_o and by transverse pitch S_T and longitudinal pitch S_L measured between tube centres.

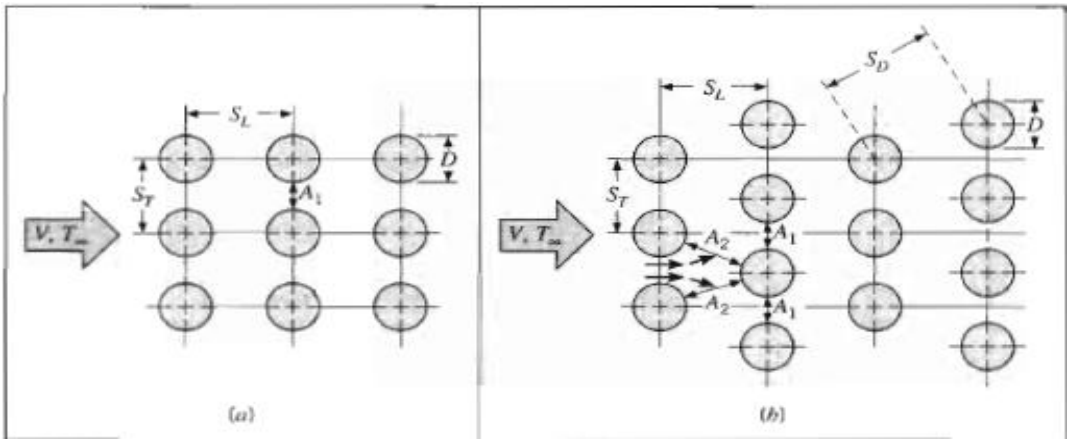

Figure 2.2: Inline and staggered tubes arrangement (Incropera and Dewitt, 2002)

The heat transfer coefficient associated with a tube is determined by its position in bank. The tubes of first few rows acts as a turbulence generating grid, which increases the heat transfer coefficient for tubes in the following rows. Grimison, 1937 gave the relation for average heat transfer coefficient for air flow through entire tube bundle as:

$$Nu = C_1 Re^m \qquad \begin{cases} N_L \geq 10 \\ 2000 \leq Re \leq 40000 \\ Pr = 0.7 \end{cases}$$

Where, C_1 and m are constants.

This relation can be used for other fluids as:

$$Nu = 1.13 C_1 Re^m Pr^{1/3} \qquad \begin{cases} N_L \geq 10 \\ 2000 \leq Re \leq 40000 \\ Pr \geq 0.7 \end{cases}$$

All the properties appearing in the above equations are evaluated at the film temperature. If N_L<10 a correlation factor may be applied such that:

$$Nu_{N_L<10} = C_2 Nu_{N_L \geq 10}$$

Where C_2 is constant.

For the aligned arrangement, V_{max} occurs at the transverse plane A_1 and from the mass conservation, it is given as:

$$V_{max} = \frac{S_T}{(S_T - D) \times V}$$

For staggered configuration maximum velocity may occur at transverse plane A_1 or at diagonal plane A_2. It will occur at A_2 if the rows are spaced such that $2(S_D\text{-}D)<(S_T\text{-}D)$ in which case it is given as:

$$V_{max} = \frac{S_T}{2(S_D - D) \times V}$$

If V_{max} occurs at A_1 for staggered configuration it may be computed from V_{max} relation given for aligned arrangement.

Zhukuskas has proposed the correlation as:

$$Nu = CRe^m Pr^{0.36} \left(\frac{Pr}{Pr_s}\right)^{1/4} \qquad \begin{cases} N_L \geq 20 \\ 0.7 \leq Pr \leq 500 \\ 1000 \leq Re \leq 2 \times 10^6 \end{cases}$$

Where all properties except Pr_s are evaluated at mean of fluid inlet and outlet temperatures. If $N_L<20$, a correction factor may be applied such that:

$$Nu_{N_L<20} = C_2 Nu_{N_L \geq 20}$$

The power required to move the fluid across the bank affects the operating cost and is directly proportional to the pressure drop which may be expressed as:

$$\Delta p = N_L \chi \left(\frac{\rho {V_{max}}^2}{2}\right) f$$

Chilton and Generaux, 1934 studied relative spacing effects of tube on pressure drop coefficient in laminar region, but Chilton and Generaux did not show any dependency of pressure drop coefficient in turbulent regime. Exponent of Reynolds number and arrangement factor was measured by Brandt, 1934. Brandt showed the dependence of exponent of Reynolds number on longitudinal spacing and relative transverse for inline tube configuration. Zukauskas, 1968 has done experimental analysis and developed some graphs which showed the relation of pressure drop between turbulent and transitional regime. The equation of staggered arrangement of tube bundles with narrow cross section with direction of flow being perpendicular was derived by Kast, 1974. Superpositon of laminar and turbulent flow was done. Charts for inline and staggered tube bundles were given.

A correlation for fully developed turbulent flow for the range of 10^4<Re<10^5 and 0.5<Pr<2000 is given by Petukhov and Popov, 1963. Boundary condition applied for following correlation is constant heat flux.

$$Nu = \frac{\frac{f}{2} \times Re \times Pr}{(1 + 136f) + \left(11.7 + 1.8Pr^{\frac{1}{3}}\right) \times \left(\frac{f}{2}\right)^{\frac{1}{2}} \times \left(Pr^{\frac{2}{3}} - 1\right)}$$

where $f = (3.64log_{10}Re - 3.28)^{-2}$

Petukhov and Kirillor, 1970 also given a correlation,

$$Nu = \frac{\frac{f}{2} \times Re \times Pr}{1.07 + 12.7 \times \left(\frac{f}{2}\right)^{\frac{1}{2}} \times \left(Pr^{\frac{2}{3}} - 1\right)}$$

The range for the above equation is 10^4<Re<10^6 and 0.5<Pr<200.

In smooth tubes fully developed turbulent flow was examined by Webb, 1971. The range for the following equation is $0.1<Pr<10^4$ and $10^4<Re<10^6$.

$$Nu = 5.0 + 0.015 \times Re^m \times Pr^n$$

where, $$m = 0.88 - \left(\frac{0.24}{4+Pr}\right), n = \left(\frac{1}{3}\right) + 0.5 \times 0.5^{(-0.6Pr)}$$

The correlation given by Gienlinski, 1976 covered a lower Reyonlds number range ($2300 \leq Re \leq 5 \times 10^6$). This correlation was the modification of Petukhov-Kirillor correlation.

$$Nu = \frac{\left(\frac{f}{8}\right)(Re - 1000)Pr}{1 + 12.7\left(\frac{f}{8}\right)^{0.5}(Pr^{2/3} - 1)}$$

2.6 CFD modeling

CFD is a computational technique to solve the fluid flow and heat transfer problems. This technique is very powerful and widely used.

The integral form of generic transport equation governing fluid flow and heat transfer can be expressed as (Versteeg and Malalasekera, 1995):

$$\frac{\partial}{\partial t}\int_\Omega \rho\phi d\Omega + \int_S \phi\rho V.dA = \int_S q_\phi.dA + \int_\Omega q_\phi \, d\Omega \qquad (1)$$

Most of the industrial heat transfer problems are in turbulent region. Hence, industrial problems are solved using turbulence model. The different approaches used for solving turbulent flows are given below.

Turbulence Modelling Scheme

Turbulent Flows:

Turbulent flows are normally seen in wide range of natural and engineering systems. Main features of turbulent flows are:

- Turbulent flows are three dimensional, diffusive and highly unsteady.
- Fluctuations are very high in turbulent flows which makes direct numerical simulation of turbulent flows very difficult.

Numerical simulation of turbulent flows:

Three approaches for prediction of turbulent flows have emerged in numerical simulation:

- Reynolds Averaged Navier-Stokes (RANS) simulation
- Large Eddy Simulation (LES)
- Direct Numerical Simulation (DNS)

Reynolds Averaged Navier-Stokes Simulation:

RANS simulations are based on time averaging of Navier-Stokes equations. New terms appear in governing equations which are modelled to ensure closure. The requirement of very fine grids is reduced by modelling. RANS simulations are widely used in industrial CFD for design analysis.

Standard k- ε model:

The standard *k-ε* model proposed by Launder and Spalding (1974) makes use of two model equations, one for turbulent kinetic energy, k and one for rate of dissipation of turbulent kinetic energy per unit mass, *ε*. These equations are;

$$\frac{\partial(\rho k)}{\partial t} + \frac{\partial}{\partial x_j}\left(\rho k v_j\right) = \frac{\partial}{\partial x_j}\left[\frac{\mu_T}{\sigma_k}\frac{\partial k}{\partial x_j}\right] + 2\mu_T S_{ij} S_{ij} - \rho\mathcal{E} \qquad (2)$$

$$\frac{\partial(\rho\mathcal{E})}{\partial t} + \frac{\partial}{\partial x_j}(\rho\mathcal{E} v_j) = \frac{\partial}{\partial x_j}\left[\frac{\mu_T}{\sigma_\mathcal{E}}\frac{\partial\mathcal{E}}{\partial x_j}\right] + C_{1\mathcal{E}}\frac{\mathcal{E}}{k}\,2\mu_T S_{ij} S_{ij} - 2C_{2\mathcal{E}}\rho\frac{\mathcal{E}^2}{k} \qquad (3)$$

These equations are iteratively solved with Reynold Averaged Navier Stokes equations.

a) Continuity equation

$$\frac{\partial \rho}{\partial t} + \frac{\partial (\rho u_j)}{\partial x_i} = 0 \qquad (4)$$

b) Momentum equation:

$$\frac{\partial (\rho u_i)}{\partial t} + \frac{\partial (\rho u_i \rho u_j)}{\partial x_i} = \frac{\partial}{\partial x_j}\left[\rho \delta_{ij} + \left(\frac{\partial u_i}{\partial x_j} + \frac{\partial u_j}{\partial x_i}\right)\right] + \rho g_i \qquad (5)$$

c) Energy equation:

$$\frac{\partial (\rho C_p T)}{\partial t} + \frac{\partial (\rho u_i C_p T)}{\partial x_i} - \frac{\partial \left[\lambda \frac{\partial T}{\partial x_j}\right]}{\partial x_j} = S_T \qquad (6)$$

The five adjustable coefficients involved in k- ε equations were given as, (Versteeg and Malalasekera, 1995);

C_μ=0.09, σ_k=1.3, σ_ε=1.3, $C_{1\varepsilon}$=1.44, $C_{2\varepsilon}$=1.92

2.7 Previous Research Work

The literature based on previous work carried out on the design, analysis and optimization of tubular cross flow heat exchangers has been studied and presented in the following text.

Chumpia and Hooman (2014) have studied the effects of heat transfer performance and pressure drop characteristics on aluminium foam wrapped tubular heat exchanger. Five samples of aluminium foam wrapped tubes with varying thickness of foam and air velocity, the heat transfer rate, overall thermal resistance and pressure drop on each sample is evaluated. The smaller is the foam layer thickness and the higher is the thermal resistance. As reported by Chumpia and Hooman and examined by angirasa and mancin et al., it has been found that thermal glue bonding has Thermal Contact Resistance (TCR) between 10% and 19%, corresponding to the velocity in this analysis of the total thermal resistance. Despite the

disadvantage, the foam still performs considerably better than the same thickness of fin. Higher the thickness and higher is the pressure drop, while those with the lowest thickness generate minimum pressure drop. Higher the thickness and higher is the heat transfer of foamed tube when compared to same thickness of finned tube. Overall thermal resistance decreases with the of foam layer thickness.

Toolthaisong and Kasayapanand (2012) have studied the air side heat transfer and pressure drop characteristics at steady state for cross flow heat exchanger having flat tube configuration with staggered arrangement by varying attack angles and aspect ratio with velocity variation. At an attack angle of 90^o, heat transfer rate and pressure drop is maximum at a given aspect ratio with increase in velocity and as the aspect ratio increases the heat transfer rate and pressure drop decreases at a given attack angle with increase in velocity. The thermal hydraulic performance of all the aspect ratio has decreased with increase in air velocity and attack angle. The maximum thermal hydraulic performance occurred on the 0^o of each tube aspect ratio while 90^o gives minimum thermal hydraulic performance.

Pongsoi et al. (2012) have studied the effects of air-side performance of crimped spiral fin and tube heat exchangers at high Reynolds numbers (3000-13000). The test heat exchanger have a new type of multi pass parallel and counter cross flow arrangements. The test samples are made from copper and aluminium with different number of rows. The results show that there is no significant effect for either number of tube rows or fin material on heat transfer performance which is found at high Reynolds no. Analysis of air-side heat transfer and friction characteristic of all the heat exchangers examined are presented in the terms of calburn factor and friction factor against Reynolds no. It has been seen that calburn factor and friction factor decreases with increase in Reynolds no. but number of tube rows cast no significant effect on calburn factor and friction factor at high Reynolds no. It has been seen

that number of tube rows doesn't affect fin efficiency, because efficiency depends upon fin material, shape and size. It has been seen that pressure drop and heat transfer rate increases with increase in number of tube rows.

Ishak et al. (2013) have studied heat transfer and pressure drop characteristics of air flow in a staggered flat tube bank in a cross flow with laminar forced convection. Experiments have been performed by varying the air velocity, Reynolds number and total heat flux and their effects on nusselt number have been seen. It has also been observed that the pressure drop increases with increase in Reynolds number. Mean Nusselt number increases with increase in Reynolds number with all heat flux supplies. The average heat transfer coefficients for the flat tube bundles depend on the mean free stream velocity of the air and the heat flux supply. The heat transfer rate increases with the increase in mean air velocity.

Du. et al. (2013) have studied the heat transfer and resistance characteristics of two finned oval- tube heat exchanger. Four meet angles (90^o, 60^o, 45^o and 30^o) are investigated separately to acquire the heat transfer and pressure drop performances by varying Reynolds no. The correlation of for two finned oval tube heat exchangers are obtained under four different air inlet angles. It has been found that the inclined air inlet angle has completely different effects on the overall performance for different heat exchangers. For the optimum performance of a finned oval tube heat exchanger, there must be an optimum inlet angle, considering the heat transfer, pressure drop, space usage, economic performance, etc.

Sano et al. (2011) have studied the effects of thermal dispersion on heat transfer and temperature field with in cross flow tubular heat exchanger both analytically and numerically. It has been noticed that thermal dispersion caused by fluid mixing due to the presence of obstacles has significant effect on the enhancement of heat transfer. Therefore it must be taken into account for accurate estimation of exit temperature and total heat transfer rate. It

has been found that the relationship between interstial heat transfer coefficient and longitudinal thermal dispersion conductivity is inverse proportional. The results obtained from the numerical simulation and analytical calculations closely follow the temperature development obtained. This study shows that the conventional estimations without considerations of thermal dispersion results in error in fluid temperature development and underestimation of total heat transfer rate.

Dixit and Ghosh (2013) studied thermal interactions of heat exchanger fluids with the surroundings. It is necessary to determine the effect of these interactions on exchanger performance when the demand of heat exchanger effectiveness is very high, like in case of cryogenic applications. In this study, effect of heat in leak in two streams cross flow exchangers has been studied and compared with the two other types of flow arrangements, namely counter current and co current. Mathematical model involving mutual heat exchange between hot and cold fluid streams and their individual thermal interactions with ambient have been considered through overall heat transfer coefficients. Various heat exchange possibilities depending on the relative temperature difference between fluids and ambient have been considered.

Heat exchanger performance defined in terms of hot and cold fluid effectiveness may have different indications. As for example, when both the hot and cold fluids are colder than ambient temperature, the hot fluid effectiveness is inversely proportional to heat in-leak while the cold fluid effectiveness shows direct proportionality to the heat ingress. Performance of balanced cross-flow heat exchanger is in between that of counter-current and co-current units under similar external thermal interaction. When the ambient thermal resistance is extremely low, the cross flow heat exchanger tends to come in equilibrium with the surrounding. Similar behavior has also been noticed with co-current and counter-current heat exchangers.

The relative temperature difference between ambient and hot (or cold) fluid decides the direction of heat exchange. Heat exchanger performance depends significantly on the direction.

Buckinx et al. (2013) formulates a design method for small scale parallel plate cross flow heat exchangers which takes wall conduction effects into account. It is shown that when the characteristic length scales of the channels are reduced at a constant pressure drop, the effectiveness exhibits a maximum due to axial heat conduction in the plate material. The point of maximal effectiveness is found to correspond to a maximal thermal power density and thus to the minimal volume required for obtaining a given effectiveness. Recently research affirmed that the phenomenon of wall heat conduction significantly deteriorates the performance of small scale heat exchangers. The mathematical model for the effectiveness and power density of the cross-flow heat exchanger is based on the temperature distributions of both fluids and the separating wall plate in between. An in house finite volume code was used to solve the differential equations for the temperature distributions and to calculate the effectiveness numerically. The final result of this study consists of closed-form expressions for the optimal plate length and plate distance for a symmetric balanced cross-flow heat exchanger. The designer has to impose pressure drop and effectiveness as constraints and has to prescribe the fluid and material properties as well as the relative plate thickness. The imposed design effectiveness therefore determines the optimal relative plate spacing. The optimal plate length is also determined by the point where the maximum effectiveness equals the desired design effectiveness.

Aquaro and Pieve (2007) gave an overview of recent high temperature heat exchangers technology developments, both in the thermal-fluid dynamic innovative solutions and in the materials. Gas turbine recuperative cycles, microturbine systems, indirectly fired cycles and

high temperature gas cooled nuclear reactors are the investigated fields where this kind of heat exchangers is used. Many industrial processes require high temperature systems, for inherent reasons or in order to improve the efficiency. This is particularly used in the case of the power production plants. Some common technological issues are, new surface geometry requirements and the needs for improving materials performance, join all of these systems. For high-pressure gas turbine recuperators, the peculiarity of managing two highly different massive flows has been shown through a numerical example, suggesting some possible solutions. As regards the material issue three reference ranges have been identified, depending on the temperature. The nickel-based superalloys are the most promising up to 800–850 ^{o}C and also above, if a properly aimed design of microstructure and mechanical properties is planned. In this regard, Alloy 625 has to be quoted as the only superalloy that has been commercially developed and extensively used in high temperature recuperators, being selected for two different gas turbine recuperators, one by Solar Turbines and one for military purposes. Evidently, if a very ambitious target is set as for the achievable system efficiency, for instance a microturbine efficiency of 40%, then the use of ceramic materials for the recuperator would be mandatory.

Gomez et al. (2009) have thermally characterize a cross-flow heat exchanger featuring a new cross-flow arrangement, which may find application in contemporary refrigeration and automobile industries. To assess the heat exchanger performance, it is compared against that for the standard two-pass counter-cross-flow arrangement. The two-part comparison is based on the thermal effectiveness and the heat exchanger efficiency for several combinations of the heat capacity rate ratio, C*, and the number of transfer units, NTU. The proposed new flow arrangement delivers higher thermal effectiveness and higher heat exchanger efficiency, resulting in lesser entropy generation over a wide range of C* and NTU values. The procedure consists of a sequence of three basic steps: (i) division of the heat exchanger in a

finite number of three-dimensional control volumes or elements, each element being itself a mixed-unmixed cross-flow heat exchanger; (ii) solution of the set of governing equations for each element; and (iii) step-by-step solution of the governing equations of subsequent elements along each circuit of the in-tube fluid. In the above computational procedure a typical element consists of a cross-flow heat exchanger with the in-tube fluid mixed and the external fluid unmixed. Generally, the in-tube fluid is considered as the hot fluid for analysis purposes. The number of elements along the in-tube fluid circuit must be sufficiently large so that the element size remains small. This equation was derived taking into account the irreversibility caused by a finite temperature difference only. In both arrangements, air has been considered as the external fluid.

Staton and Cavagnino (2008) deals with the formulations used to predict convection cooling and flow in electric machines. Flow network analysis is used to study the ventilation inside the machine. This paper provides guidelines for choosing suitable thermal and flow network formulations. Most of the formulations are empirical based and in terms of dimensionless numbers. This gives benefits in terms of maximum reuse of the relationships developed, i.e., the same formulation can be used for similarly shaped geometries with a size that is different from that of the original experiments and/or with a different fluid. This paper can be considered as a reference that brings together useful formulations for calculating convection and flow in electrical machines.

Farsane et al. (2000) aimed at the optimization of the external surface of an induction motor of closed type and is carried out experimentally by considering, in parallel, the thermal aspects and flow distribution around the motor casing. Three non intrusive methods of investigation are used: determination of wall temperature fields by infrared thermography, flow visualization by laser sheet and measurement of velocity distribution by laser Doppler

anemometry. The results displayed overheating several zones of motor casing surface. A new configuration for motor casing has been designed and it was found that, there was significant decrease in surface temperature of casing.

Navarro and Gomez (2005) presented a new numerical methodology for thermal performance calculation in cross-flow heat exchangers is developed. Effectiveness–number of transfer units (e–NTU) data for several standard and complex flow arrangements are obtained using this methodology. The results are validated through comparison with analytical solutions for one-pass cross-flow heat exchangers with one to four rows and with approximate series solution for an unmixed–unmixed heat exchanger, obtaining in all cases very small errors. It is based on physical concepts and it is characterized by the division of the heat exchanger in a number of small and simple one-pass mixed–unmixed cross-flow heat exchangers. It is very accurate and therefore suitable for predicting the performance of several cross-flow heat exchangers, including heat exchangers with new and complex flow arrangements where analytical or approximate solutions are not disposable. It permits to obtain data for cross-flow heat exchangers configurations using the e–NTU, LMTD, P–NTU and other methods, including the obtainment of polynomial curves, graphics and correlations.

Chang et al. (2010) studied experimentally and numerically investigates the thermal performance of a large-scale motor with a capacity of 2350 kW. The large-scale motor consists of a centrifugal fan, two axial fans, a shaft, a stator, a rotor and a heat exchanger with 637 cooling tubes. The test rigs are set up to measure the performance of the fans and the temperature distributions of the motor. The models of the fan and motor have been implemented in a Fluent software package to predict the flow and temperature fields inside the motor. The calculated results show good agreement with the measured data. In order to improve the motor thermal performance, several methods have been adopted, which are

aiming to enhance the fan performance by changing the geometry, to redesign a new heat exchanger with guide vanes, and to optimize the distance between the axial fans. The modified design can decrease the temperature rise by 6^0C in both the stator and rotor.

CHAPTER 3: METHODOLOGY AND SIMULATION PROCEDURE

Heat exchangers have been used in many industries for several decades. The use of tubular cross flow heat exchangers has become popular in last few years for cooling of large electric motors. From the comprehensive literature review, it has been found that the adequate research has not been done in the field of cooling of electric motors by air cooled tubular cross flow heat exchangers. Hence, an extensive simulation procedure has been performed in order to provide some effective designs for such heat exchangers.

3.1 Methodology

Simulation on cross flow tubular heat exchanger by using commercial CFD (Computational Fluid Dynamics) code Fluent was performed using following methodology:

- Simulation has been performed on cross flow tubular heat exchanger and results are validated using experimental results for actual geometry.
- Grid independent test has been performed and optimum grid size has been found for the same geometry.
- Again, simulation has been done using different model with optimum grid size and accurate turbulence model has been obtained for the same heat exchanger.
- Then, by using the optimum grid size and turbulence model, CFD simulation is performed by changing the locations of baffles, increasing number of tubes and other geometrical parameters of heat exchangers.

- After doing the above step, best design of heat exchanger has been obtained that could maximize the rate of heat transfer at lower costs and leads to proper and uniform cooling of electric motors at lower pressure drops.
- A computer program using MATLAB programming was developed for actual geometry and results obtained from the program were compared with CFD results.

3.2 Simulation procedure

The case study done by Kumar et al., 2003 at Crompton Greves Ltd. on cross flow tubular heat exchanger has been taken for simulation using Computational Fluid Dynamics. Results obtained from CFD simulation are compared with experimental results. Further some other design changes (such as changing baffle positions, number of tubes, cold air inlet velocities, etc) have been simulated and compared with actual design. The major geometrical dimensions and simulation procedure is explained below.

Geometrical Details:

Geometry of heat exchanger was modelled in ANSYS Workbench 15.0, licenced in Thapar University using geometrical details given in table 3.1. Geometry consists of twenty seven number of tubes housed in a staggered arrangement. The bottom faces of second and third section of rectangular enclosure are inlet of hot air; whereas, the bottom faces of first and fourth section are outlets of hot air. The cold air passes through the tubes.

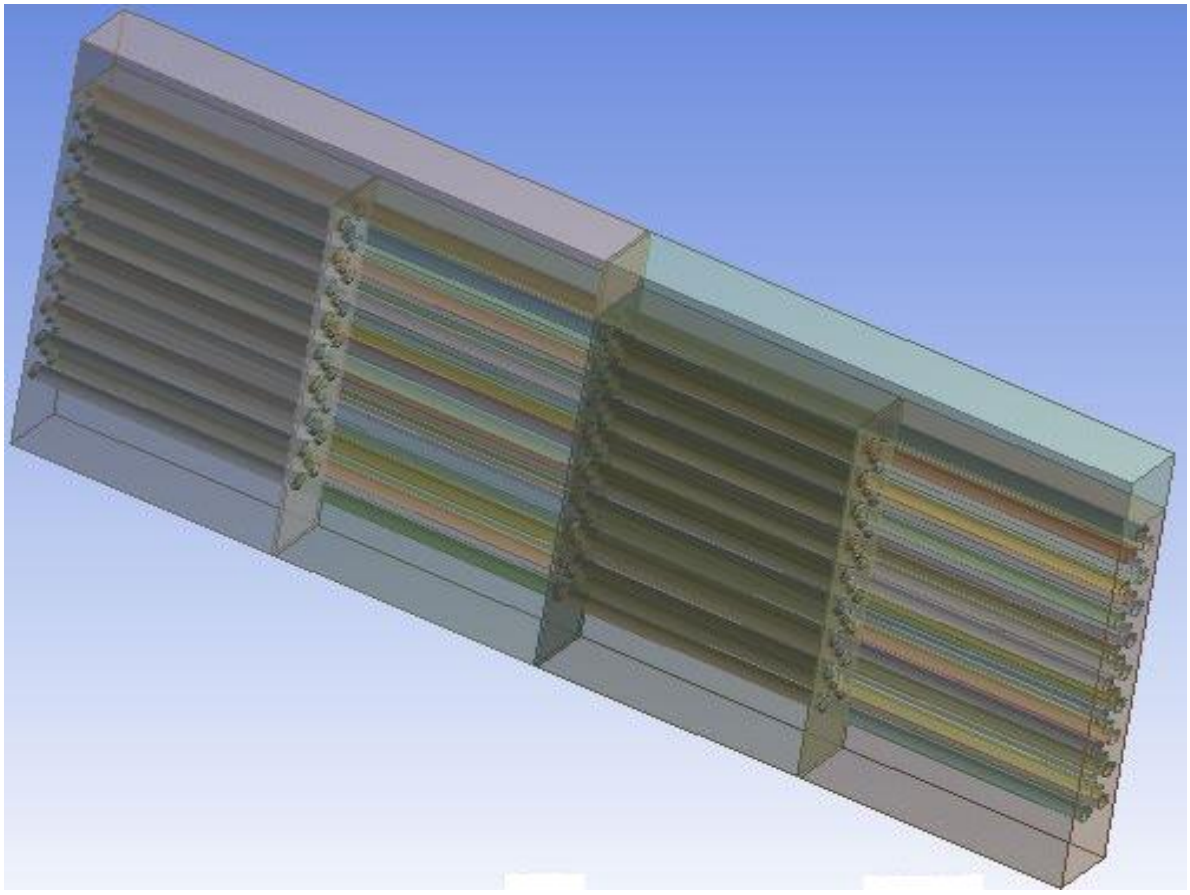

Figure 3.1: Geometry (3-D view)

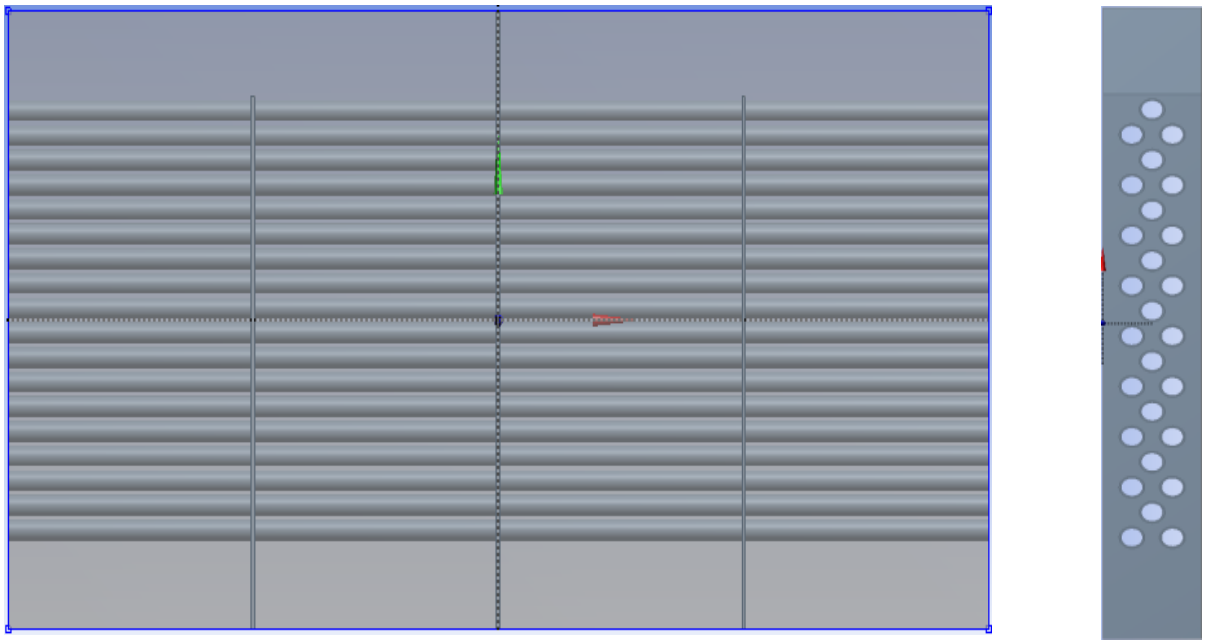

Figure 3.2: Front and side view of geometry

Table 3.1: Geometrical details

S. No.	Description	Unit	Dimensions
1.	Overall Dimension	mm	1610 x 100 x 765
2.	Inner tube diameter	mm	22
3.	Outer tube diameter	mm	26
4.	Length of tube	mm	1610
5.	Number of tubes		27
6.	Transverse pitch	mm	61
7.	Longitudinal pitch	mm	41

Modelling Assumptions:

To simulate the heat exchanger some assumptions were assumed and given below:

1. Heat leakage to surroundings and the effect of radiation losses are neglected.

2. Due to symmetry of geometrical construction of heat exchanger along its width, it is divided into two halves from the centre plane along the length. Only one half was taken for CFD simulation and symmetry boundary condition was applied along the sectioned plane.

Mesh Description:

Structured mesh was generated for the heat exchanger model. Non conformal mesh was generated for pipes and rectangular enclosure in order to decrease the total cell count which in turn effects the total computational time for the analysis. Inflation layers were

generated near the walls in order to maintain the desired y+ value. Further details of the mesh are given in table 3.2.

Table 3.2: Mesh description

Number of nodes	591023
Number of elements	543464
Average skewness	0.1847

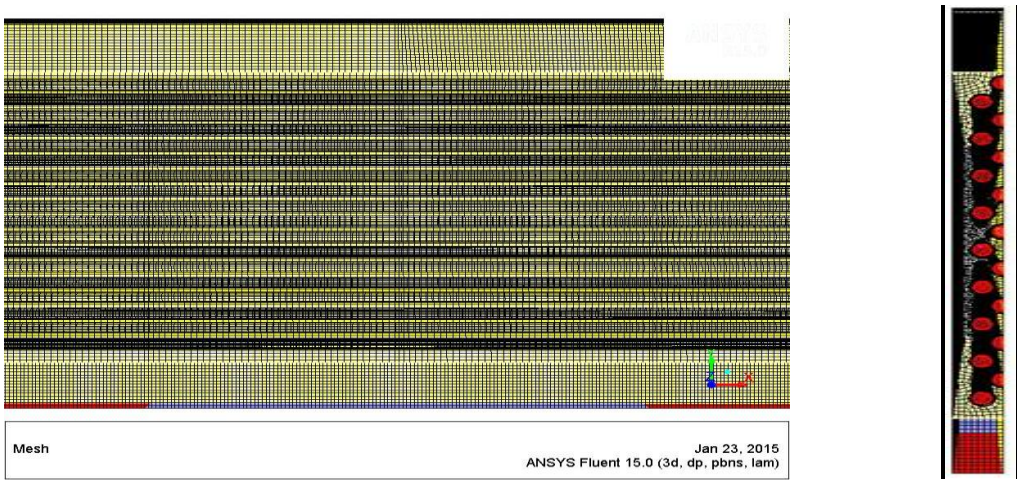

Figure 3.3: Meshed heat exchanger (Front view and side view)

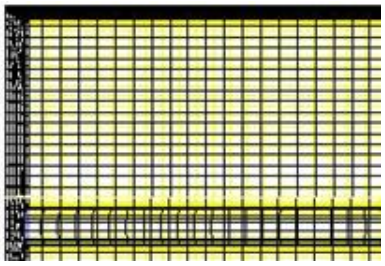

Figure 3.4: Magnified view of mesh

Properties of air and mild steel:

The hot air is coming from motor is cooled by the ambient air which is passed through the tubes of the heat exchanger. The heat exchanger is made of mild steel. Properties of hot, cold

air and mild steel used for simulation are given in table 3.3. These properties are obtained at bulk mean temperatures of both hot and cold air.

Table 3.3: Properties of Air and Mild Steel

Property	**Unit**	**Hot Air**	**Cold Air**	**Mild Steel**
Bulk Mean Temp.	K	315.88	312.04	
Density	kg/m^3	1.1086	1.121	7833
Specific Heat	J/kg-K	1007.63	1007.48	465
Thermal Conductivity	W/m-K	27.475×10^{-3}	27.191×10^{-3}	54
Dynamic Viscosity	$N\text{-}s/m^2$	192.095×10^{-7}	190.283×10^{-7}	N.A.

Boundary conditions:

Velocity and temperature of hot and cold air were specified at the inlet. The turbulent intensity at the inlet was set as 2% because geometry was symmetrical, hence less turbulence occurs. The pressure value at the outlet of both cold as well as hot fluid was specified as zero because both hot and cold air coming out of heat exchanger are at ambient pressure. The thickness of tubes and baffles is neglected during geometry modelling. To account this, shell conduction boundary condition had been taken. The values of operating parameters were specified in Table 3.4.

Table 3.4: Boundary conditions

Type of fluid	Inlet velocity (m/s)	Outlet pressure, Pa (gauge)	Inlet temperature (^{o}C)	Turbulence intensity (%)	Hydraulic diameter (m)
Cold air	18	0	35	2	0.022
Hot air	1.35	0	63	2	0.160

3.3 Description of different designs

In addition to simulation of actual design, two additional designs were obtained by changing the geometrical parameters such as location of baffles and number of tubes. All these designs were also simulated using CFD and their detailed description is given below.

Actual design:

Tubes are housed inside a rectangular enclosure, which is divided into four sections by using partition plates, internal baffles and end plates. End plates separate the hot air from the cold air. Partition plate divides the heat exchanger into two equal halves whereas internal baffles guide the path of hot air. The cold air flows through the tubes whereas the external surface of tubes is exposed to hot air. The partition plate distributes hot air in middle of two sections of heat exchanger and the cooled hot air leaves the heat exchanger from other two sections. This cooled hot air is re-circulated into the motor windings and the cold air coming out of tubes is discharged to atmosphere.

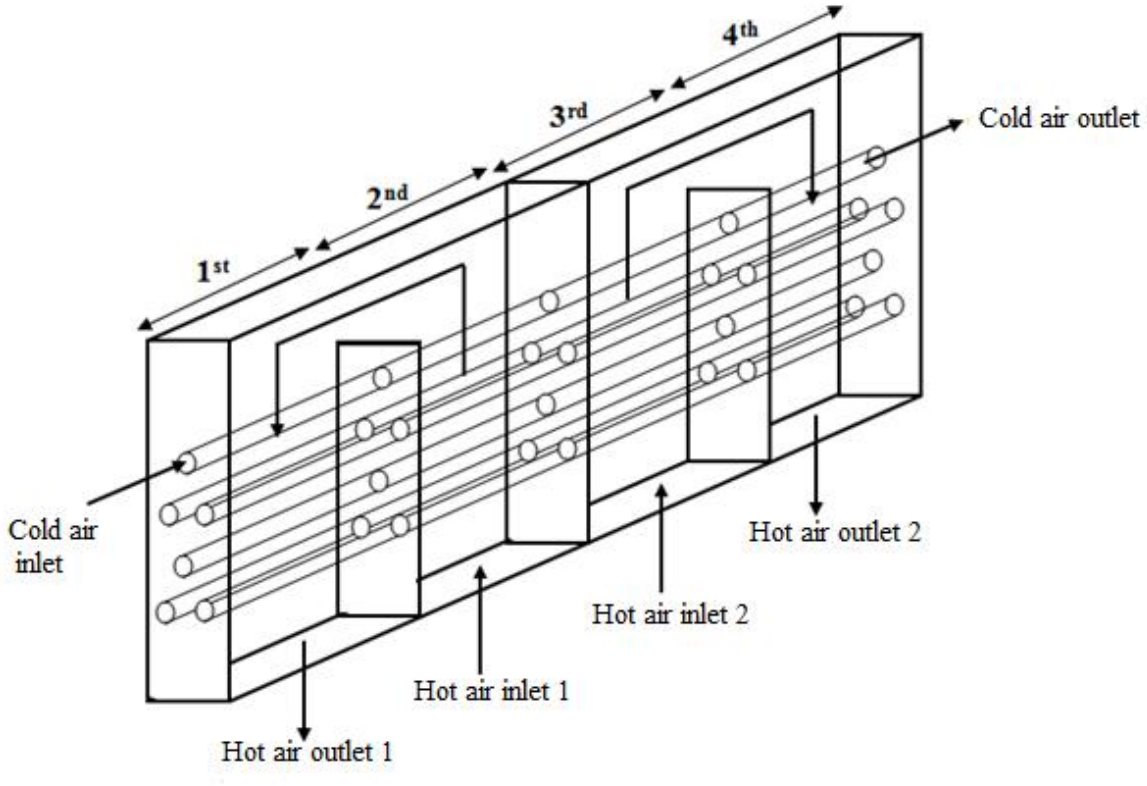

Figure 3.5: Schematic of heat exchanger

Change in baffle position:

As per the temperature drop obtained for first and second half of heat exchanger using CFD simulation, optimum ratios of heat transfer area was obtained using theoretical correlations. Based on this, area and length of tubes were obtained for each half. Central baffle has been shifted towards right by 295 mm from the central plane. Further, each half of heat exchanger is divided into two parts of equal length. The amount of hot air passed through each section was also varied in the same proportion as that of area i.e. the first section of heat exchanger has more amount of air as compared to second section. The detailed geometrical description of this design is shown in Figure 3.6.

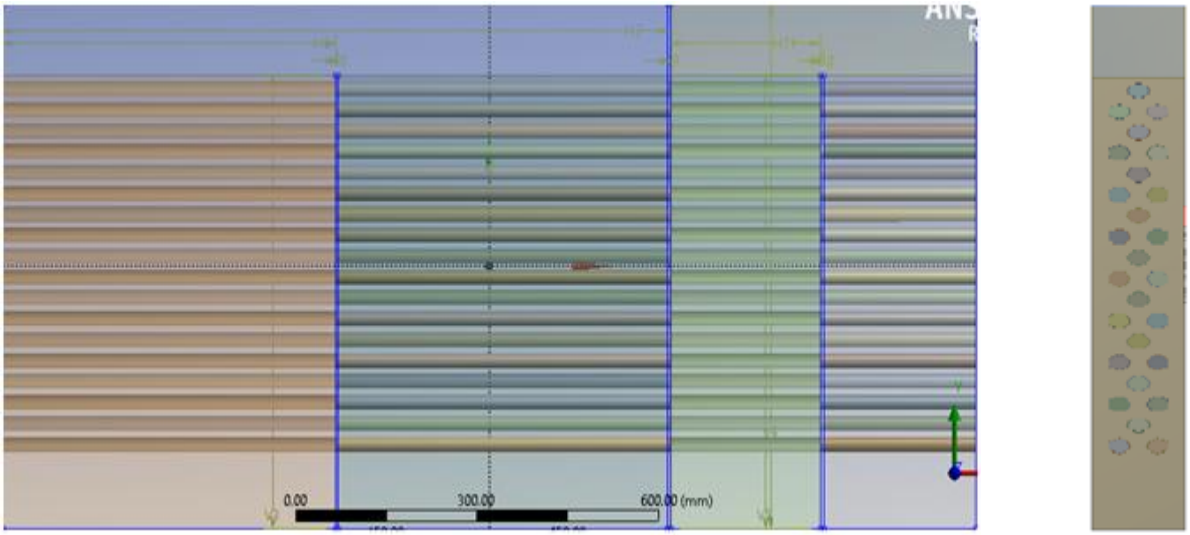

Figure 3.6: Change in baffle position design (Front view and side view)

Additional Three Tubes:

In this case, the cold air tubes has been increased from 27 tubes to 30 tubes and simulation has been carried out. Due to increase in number of tubes, heat transfer area has increased which leads to higher heat transfer rate. Detailed view of Geometry is shown Figure 3.7.

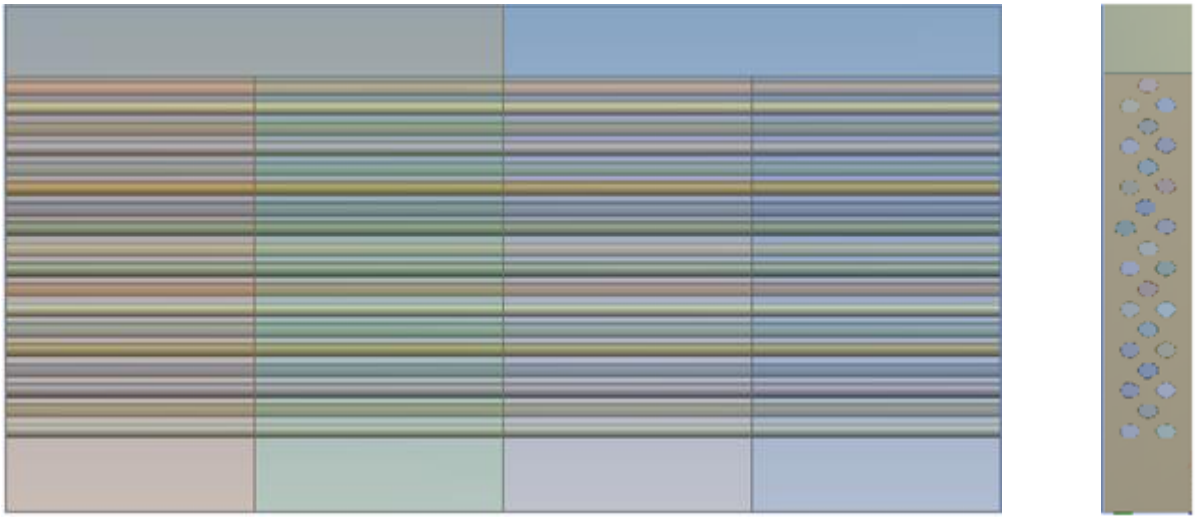

Figure 3.7: Additional three tubes design (Front view and side view)

Final design:

A final design based on the simulation results of actual model at different cold air inlet velocities and two model were suggested. From the results of velocity variation on actual model it has been found that with increase in the velocity there was not much drop in the temperature where as the pressure drop has increased drastically. Also by comparing the different designs it was observed that the addition of three tubes increases the area of heat transfer. Hence both of these effects were combined to obtain the final model which was operated at 14 m/s inlet cold air velocity with three additional tubes and the results obtained were compared with the actual model.

3.4 MATLAB programming

A program based on analytical formulation was developed for actual model. Results obtained from MATLAB program were compared with CFD simulation results at different cold air inlet velocities. A schematic of flow chart for the program is shown in Figure 3.8.

The software first evaluates the intermittent temperatures of the heat exchanger. Then it will consider the first leg of the heat exchanger and calculate the heat dissipation rate and outlet temperature of both the streams. Then taking the proper inlet temperatures, the heat dissipation rate and the outlet temperature of both the streams of second leg of the heat exchanger will be evaluated. Similarly the performance of other two legs of exchanger will be performed. Finally it totalises the heat dissipation rate of the exchanger (Gangacharyulu et al., 2004).

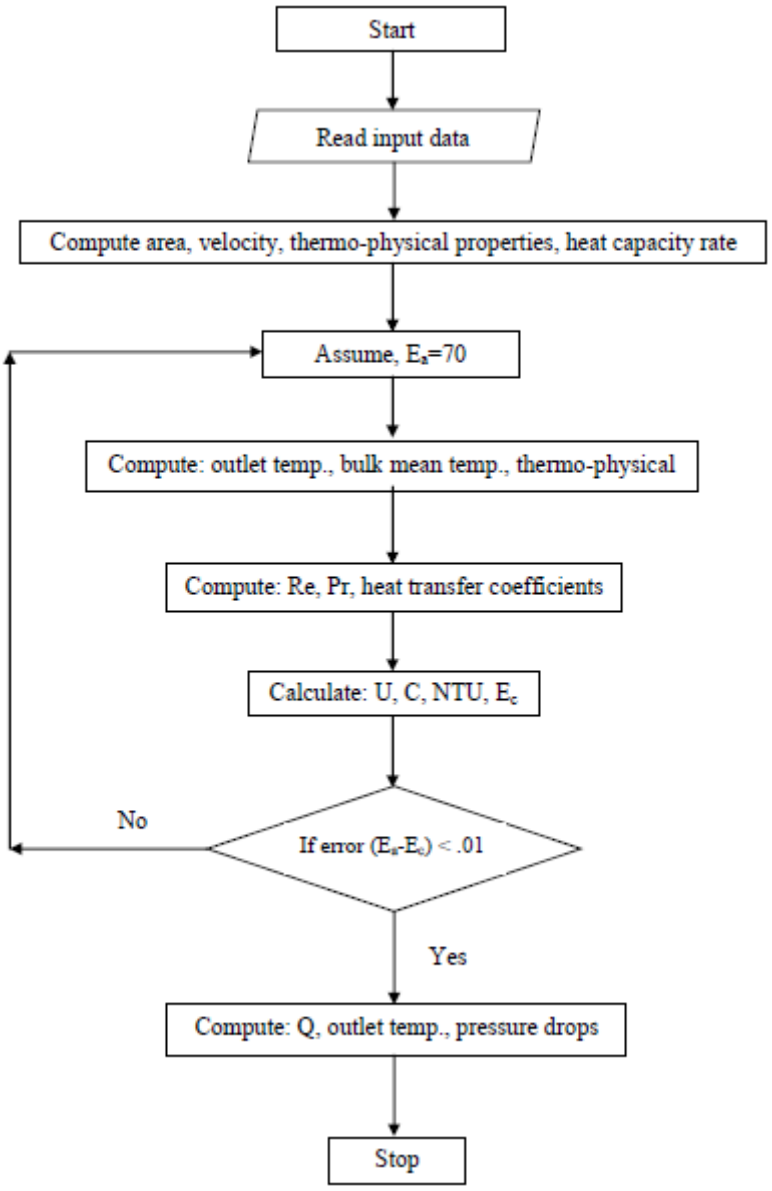

Figure 3.8: Flow chart of MATLAB program

CHAPTER 4: CFD SIMULATION RESULTS AND COMPARISION OF DIFFERENT DESIGNS

The use of tubular cross flow heat exchangers for cooling of large electric motors has been increased in past few decades using air. In spite of its applications in almost all industrial applications, not much work has been reported to date on such type of heat exchangers. So, effort has been made here, to simulate such systems using CFD and results of simulations are presented. Comparison is also made among different designs by varying the geometrical parameters.

4.1 Effect of cold air inlet velocity

Inlet velocity (mass flow rate) of cold air has been varied for actual design and its effect has been studied on outlet temperatures, heat transfer coefficient and pressure drop of hot and cold air. Inlet velocity of the cold air has been varied from 14 m/s to 20 m/s in order to study the effects on the outlet temperatures. The curves between the temperature and cold air velocity is shown in Figure 4.1 for cold and hot air outlets. It can be seen from the graph, as the inlet air velocity has increased, the temperature at all the outlets has decreased.

This is due to the fact that with increase in the velocity the heat transfer coefficient goes up which leads to increase in the heat transfer rate. A decrease of 1.83%, 2.598%, 4.78% has been found in outlet temperature of hot air outlet 1, hot air outlet 2 and cold air outlet, respectively, when velocity of cold air was varied from 14 to 20 m/s.

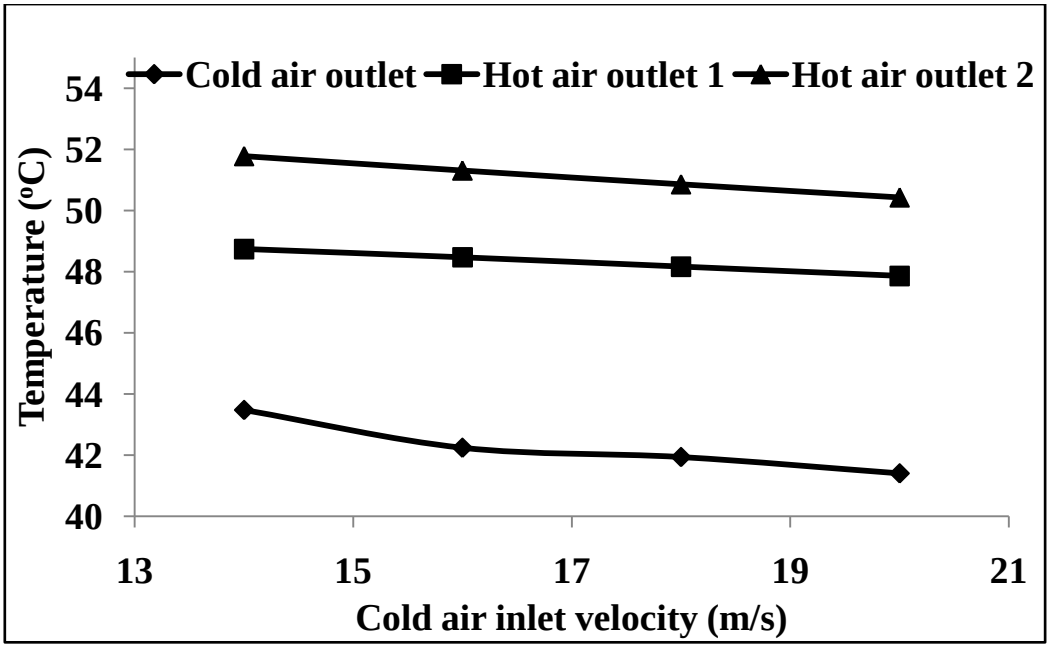

Figure 4.1: Temperature versus cold air inlet velocity

Figure 4.2, shows the variation for the pressure drop through the tubes for cold air with variation in inlet velocities.

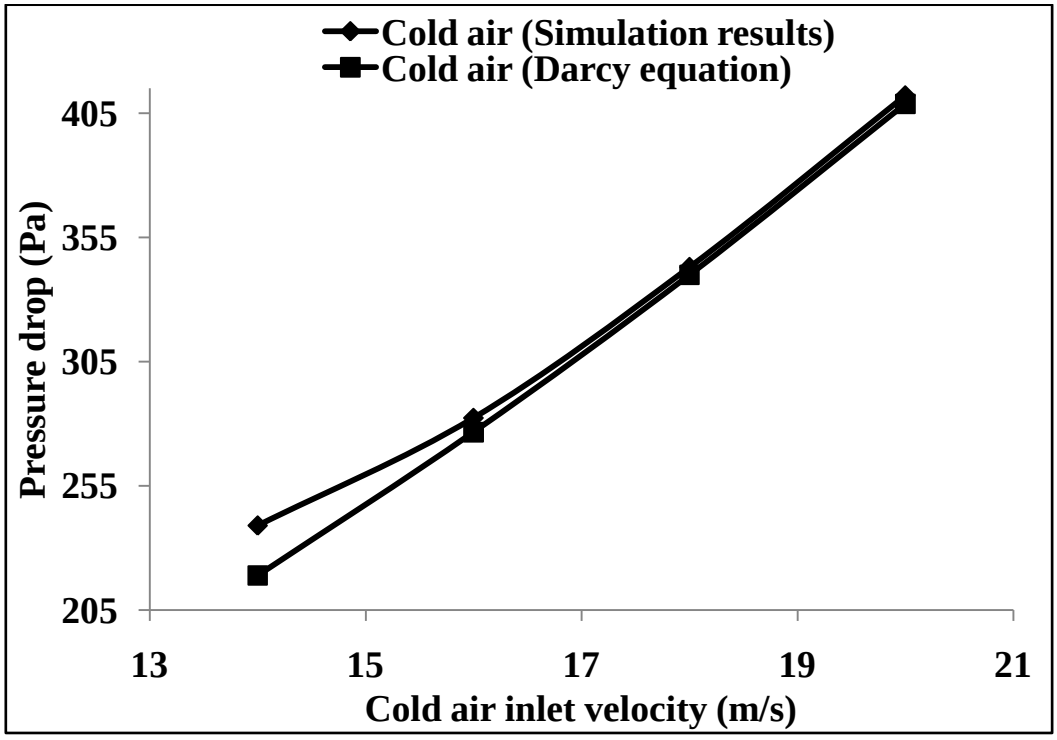

Figure 4.2: Pressure drop versus cold air inlet velocity

The pressure drop has shown a parabolic variation with increase in the inlet air velocities. This pressure drop obtained from CFD simulation has shown close agreement with theoretically obtained pressure drop. An over-prediction of 9.52% was obtained in CFD simulation results at cold air inlet velocity of 14 m/s. The pressure drop has increased by 72.39% when the inlet velocity was varied from 14 m/s to 20 m/s. It can be concluded from both the graphs that it is not worth to increase the cold air velocity because heat transfer rate is enhanced by small margin whereas huge increase in pressure drop was found which leads to increase in the requirement of pumping power and operational cost. Also, another reason for lesser temperature drop might be due to less time available for heat transfer due to increase in the velocity. The increased air velocities also leads to increase in the tube vibrations which increases the maintenance cost also.

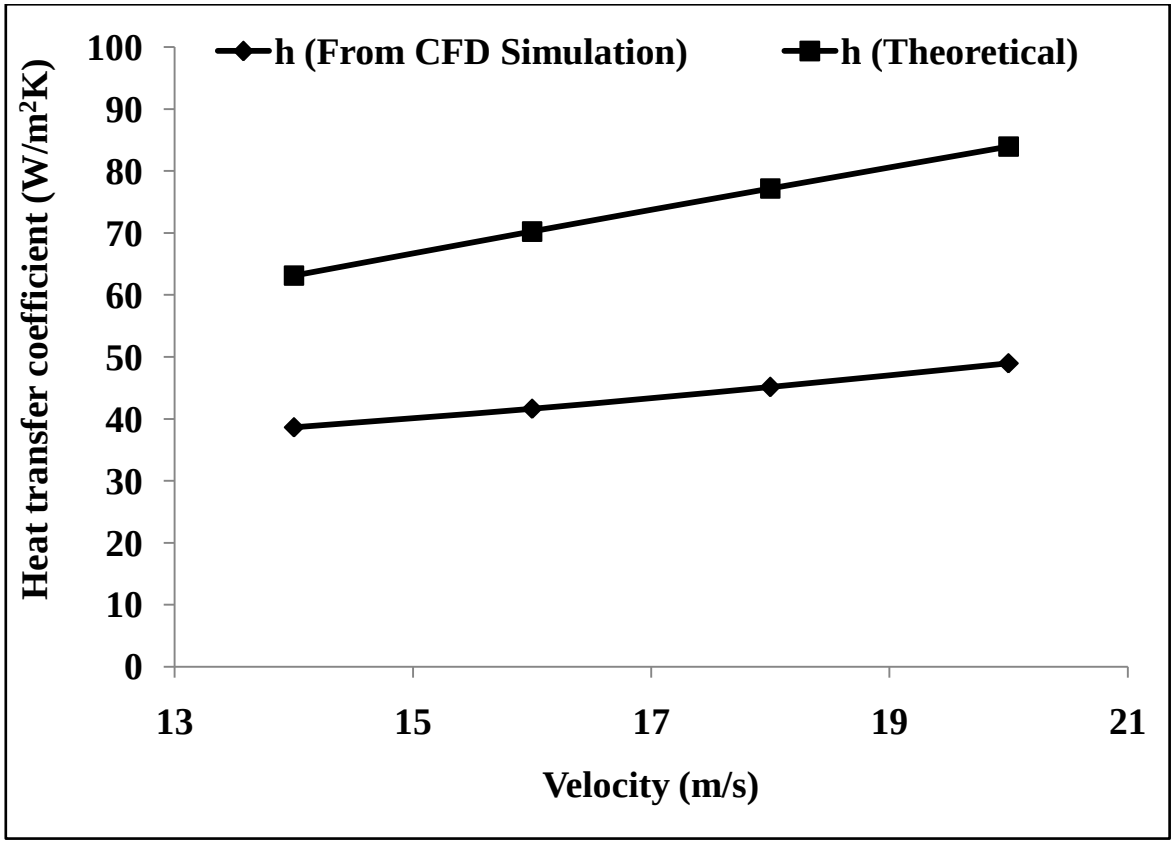

Figure 4.3: Heat transfer coefficient versus velocity

Figure 4.3, shows the variation of heat transfer coefficient with change in velocity. It can be seen from the graph that with increase in velocity there is increase in heat transfer coefficient. Both the CFD simulation curve and theoretical curve shows the same trend. A decrease of 24.82% and 21.09% was obtained for theoretical and simulated heat transfer coefficient when air velocity was decreased from 20 m/s to 14 m/s.

4.2 Comparison of different designs

Three designs were compared with the actual design by keeping all the parameters and boundary conditions fixed other than making geometrical changes. Figure 4.2 to 4.5 shows the outlet temperatures obtained for different designs.

Temperature variations:

It can be seen from Figure 4.4 that outlet temperatures at hot outlet 1 has decreased from the actual design when baffle positions has been shifted and three additional tubes were used.

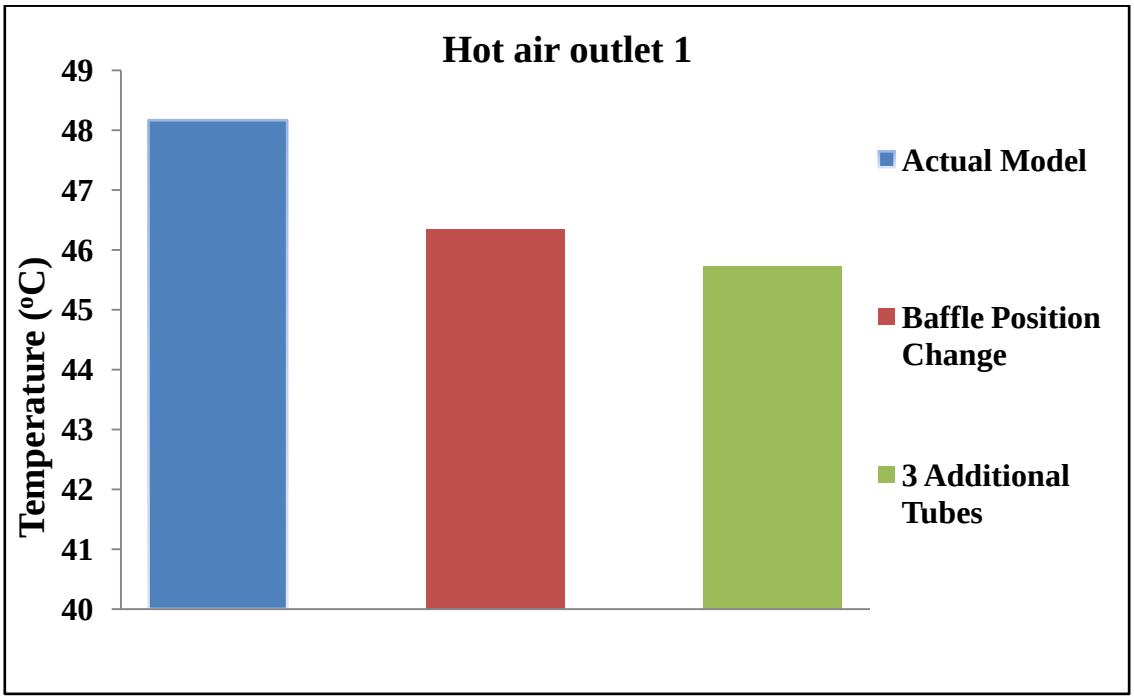

Figure 4.4: Hot air temperatures at outlet 1 for different designs

On shifting of the baffle positions the temperature has decreased due to increase in the area and time available for heat transfer. On addition of three additional tubes the area available for heat transfer has increased which causes decrease in outlet temperature of hot air.

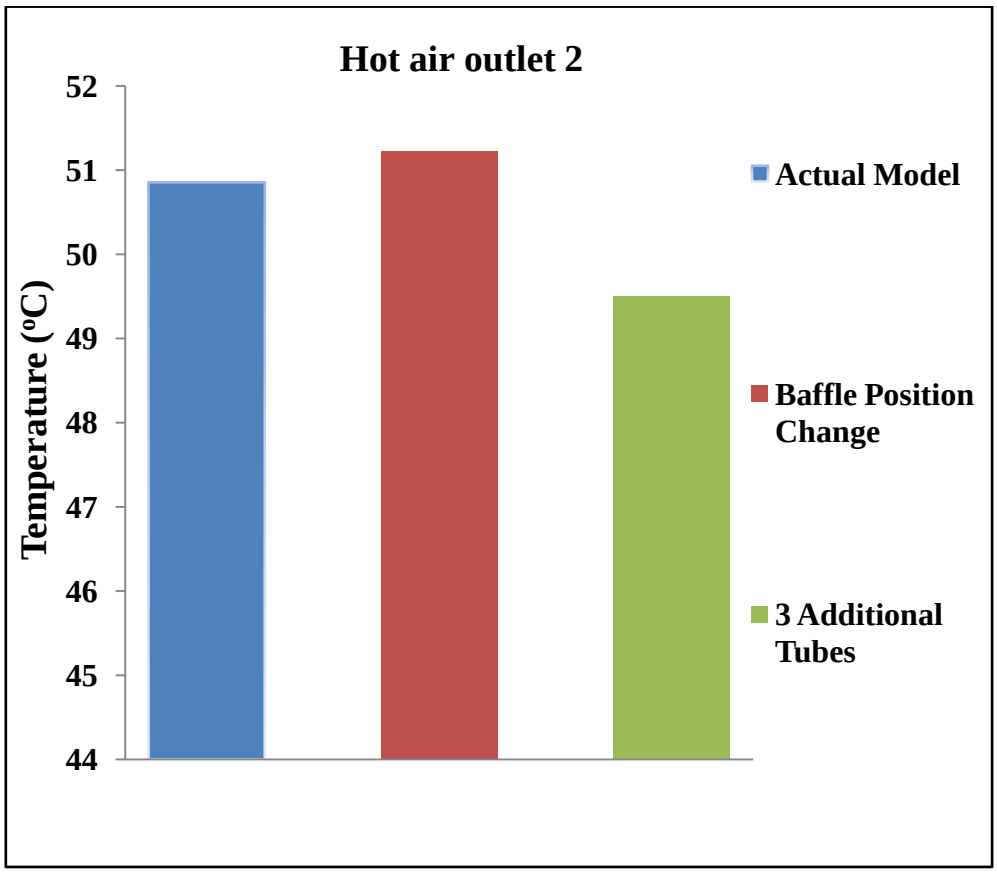

Figure 4.5: Hot air temperatures at outlet 2 for different designs

It can be seen from Figure 4.5 that, outlet temperature at hot air outlet 2 has increased due to change in the baffle position. A decrease in the hot air outlet 2 has been seen in case of three additional tubes. On shifting the baffle position the outlet temperature of hot outlet 2 has increased due to decrease in the area of heat transfer. On addition of three additional tubes, the area available for cold air heat transfer has increased because of which there is decrease in the outlet temperature at hot outlet 2.

It can be seen from Figure 4.6 that, cold outlet temperature has increased in case of three additional tubes because the heat transfer area has increased due to increase in the number of rows and hence increases rate of heat transfer.

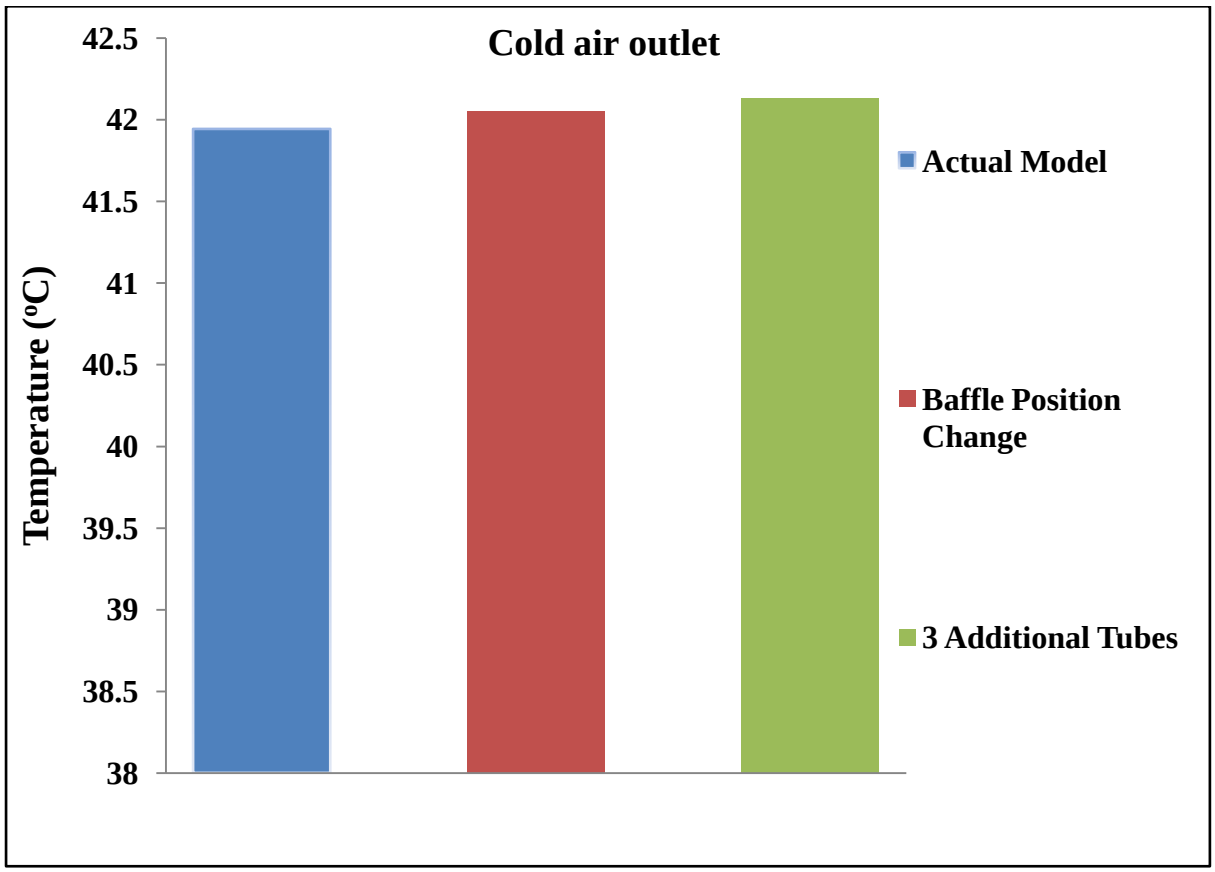

Figure 4.6: Cold air temperatures at outlet for different design

The outlet temperature of the cold air in case of change in the baffle position is almost same because the area of heat exchanger is constant irrespective of change in the baffle position.

Pressure drop variation:

Figures 4.7 to 4.9 represents the pressure drop for hot and cold air for all the designs. It can be seen from figure 4.7 that on shifting of central baffle position, the pressure drop has increased in comparison to actual design. This is because the section is handling more

amount of hot air in comparison to other designs. A marginal increase in pressure drop is also obtained on addition of three additional tubes.

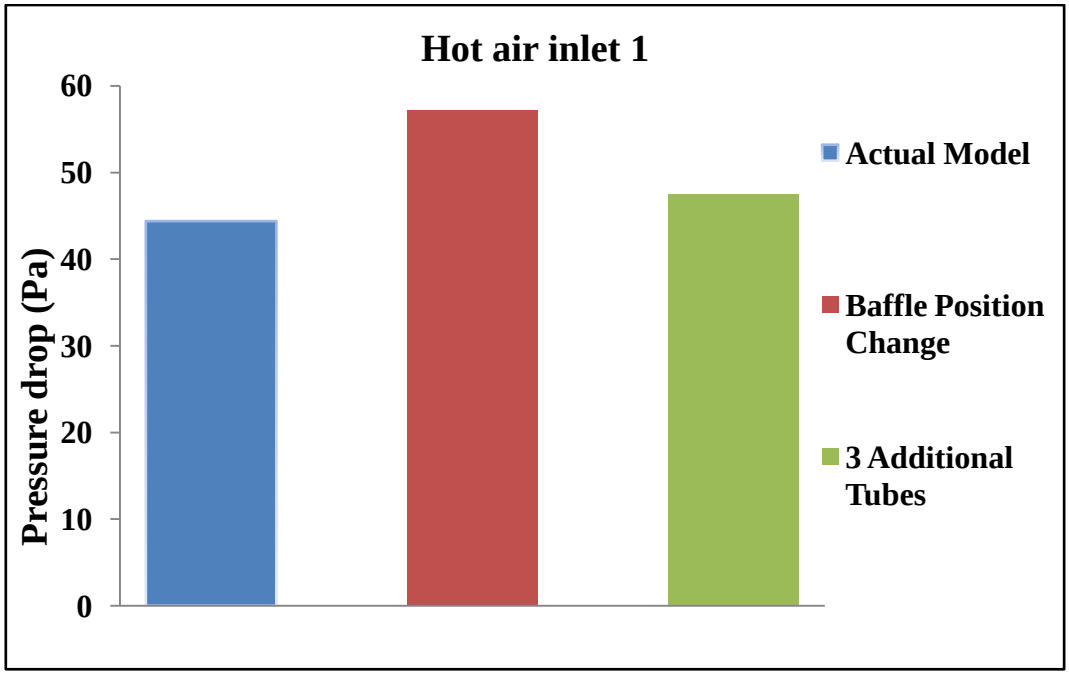

Figure 4.7: Pressure drop for first section of hot air

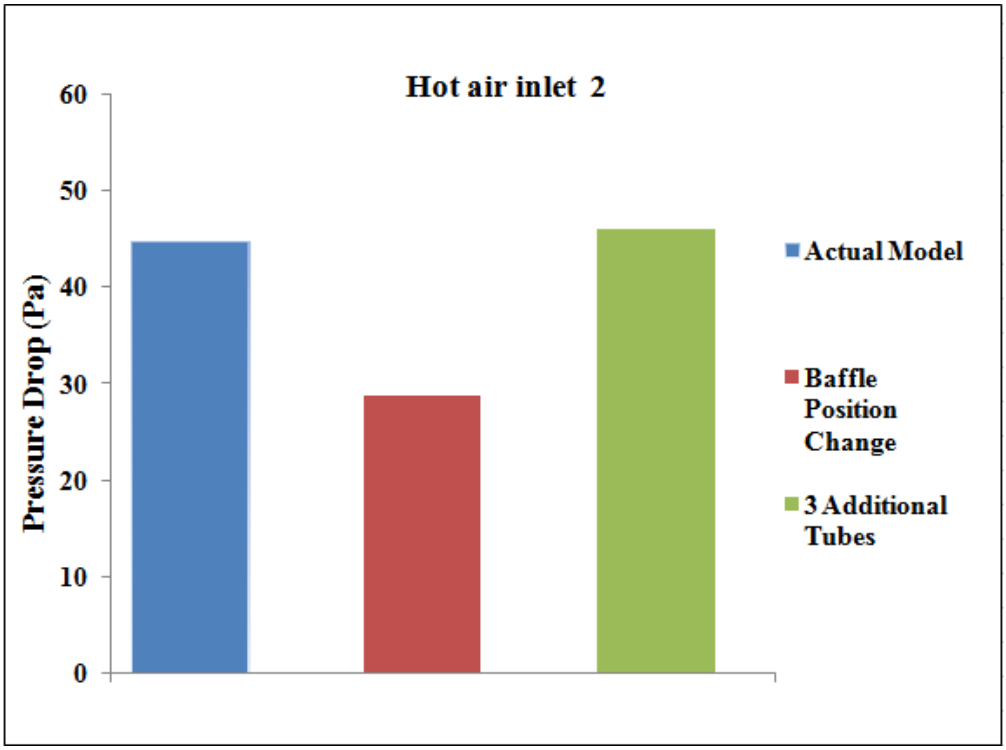

Figure 4.8: Pressure drop for second section of hot air

For second section of heat exchanger (Figure 4.8), baffle shifting model has shown minimum pressure drop because the amount of hot air for this section was very small in comparison to air handled by other models. A marginal increase has been observed in pressure drop on three additional tubes.

It is clear from Figure 4.9 that, there is not much variation in cold air pressure drop. Pressure drop has decreased for both the models. The decrease in pressure drop on addition of three tubes is obtained because, same amount of air is distributed in more number of tubes, which has decreased the air velocity in tubes and velocity has overcome the effect of additional tubes because pressure drop is directly proportional to square of velocity.

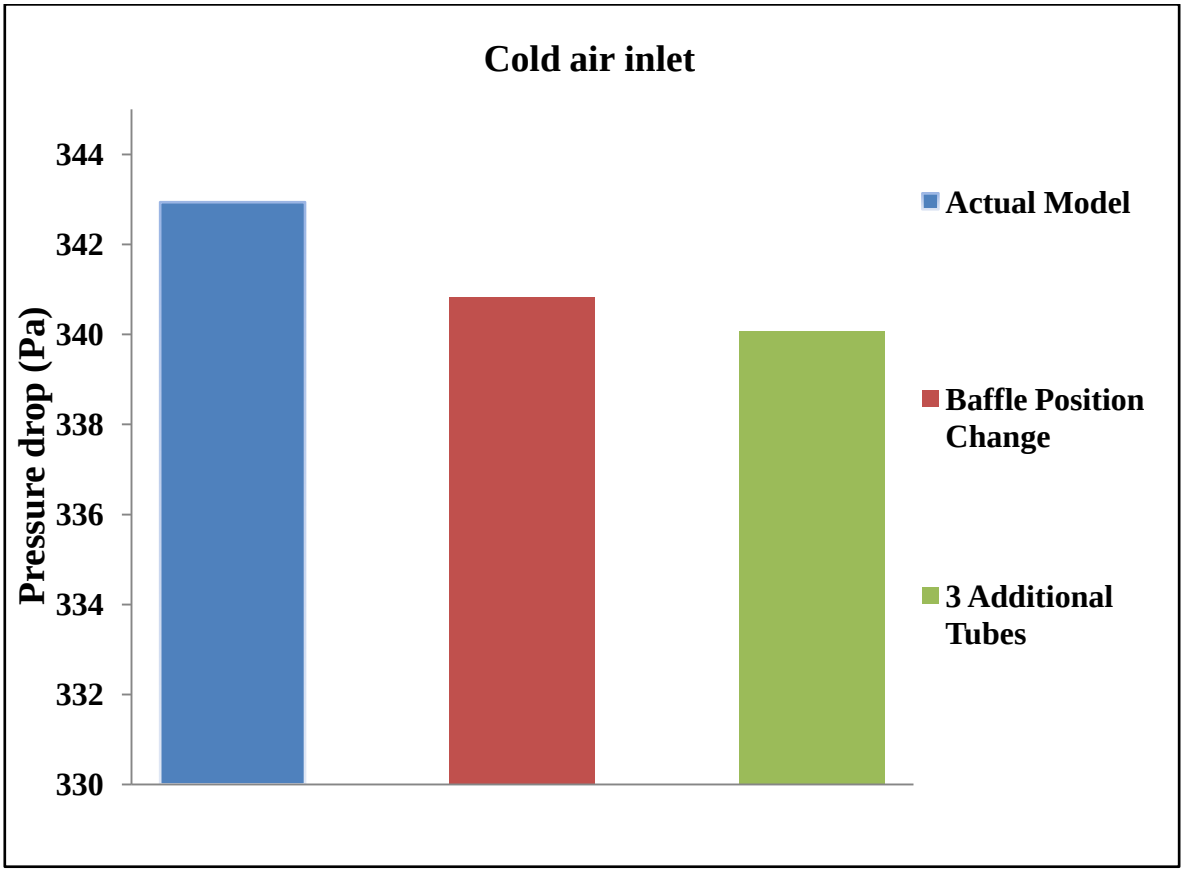

Figure 4.9: Pressure drop for cold air

4.3 Pressure and temperature distributions

Pressure distribution:

The pressure of cold fluid in the tube is higher at inlet and decreases as it moves towards outlet (Figure 4.10). The high pressure gradient along the tube length is due to friction between air and the tube wall. A small amount of negative pressure is observed nearby the outlet of cold fluid due to jet effect of cold fluid exiting from the tube.

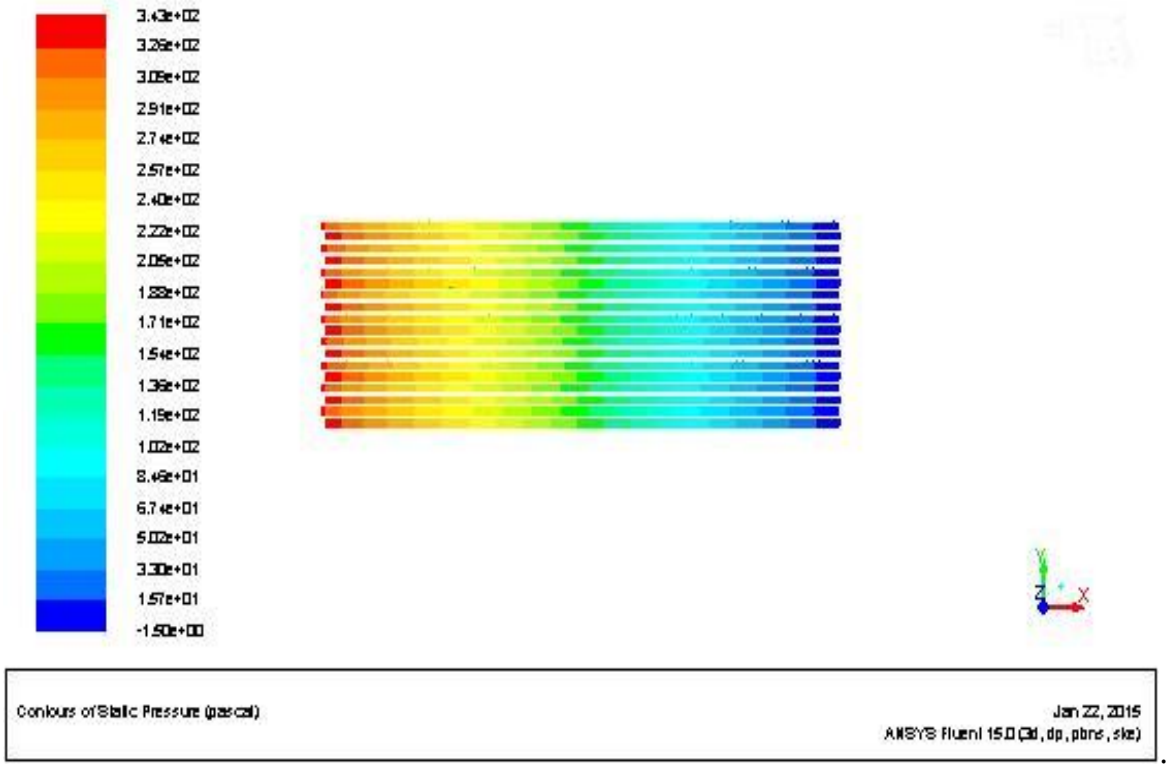

Figure 4.10: Pressure distribution of cold air

The pressure gradient is gradual in the hot stream (Figure 4.11). The pressure drop across tube bundle is about (45.30 Pa) as compared to the pressure drop in tube side along its length, which may be of the order of 342.93 Pa. At the inlet of hot air, more pressure is observed due to tube bundle and the pressure decreases, as the hot air moves up. In the second section, the pressure is low near the exit from second section to first section. The pressure decreases

from top to bottom in the first section. The similar behaviour is observed in the third and fourth section of the heat exchanger. There is appearance of high pressure zones near the top corners of first and fourth section due to stagnation of air.

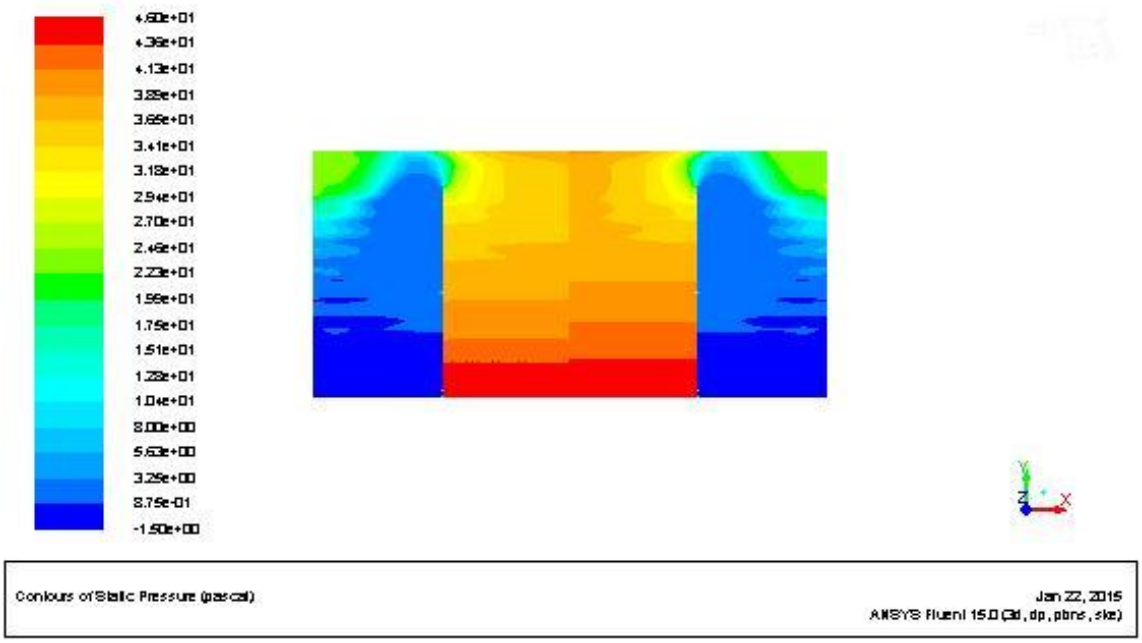

Figure 4.11: Pressure distribution of hot air

Temperature Distribution:

Fig. 4.12 shows the temperature distribution of heat exchanger in a vertical plane along its length. The temperature plot reveals that the hot air looses heat as it moves upward and the heat is gained by the cold fluid. Inside the tube, the temperature of cold air increases along its length as it picks up the heat from hot fluid while moving towards outlet. At the outlet, the exit air coming from bottom tubes are hotter than that of the exit air coming from top tubes, as the heat sources are located at the bottom.

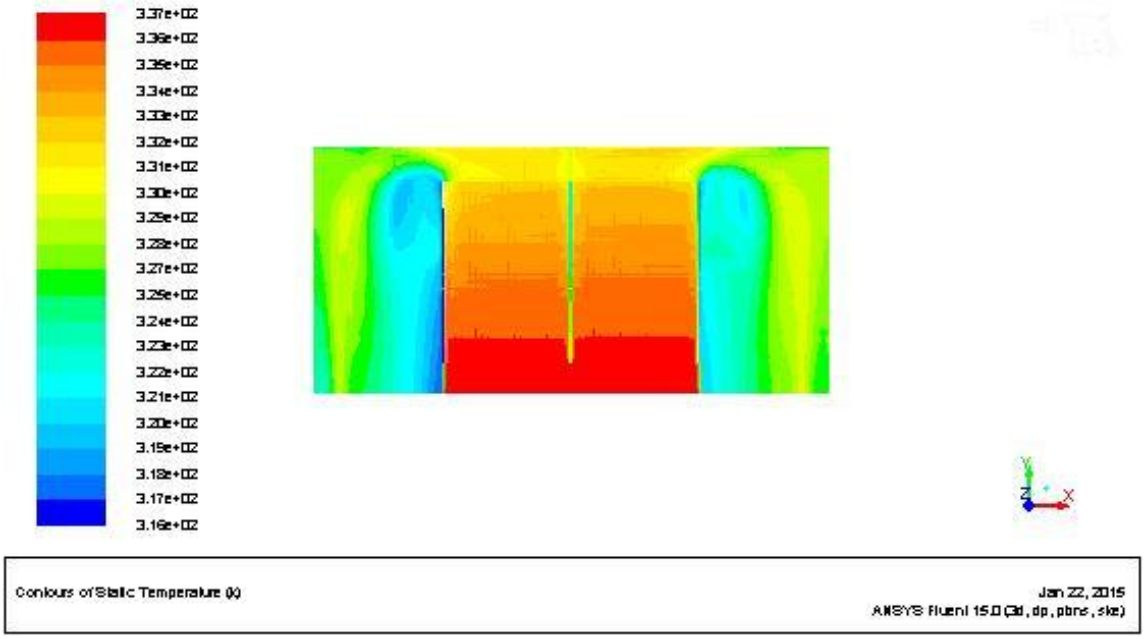

Figure 4.12: Temperature distribution of hot air

The temperature drop of hot air in the first section of heat exchanger is high (14.84 ^{o}C) because of high temperature difference between cold air and hot air (Figure 4.13).

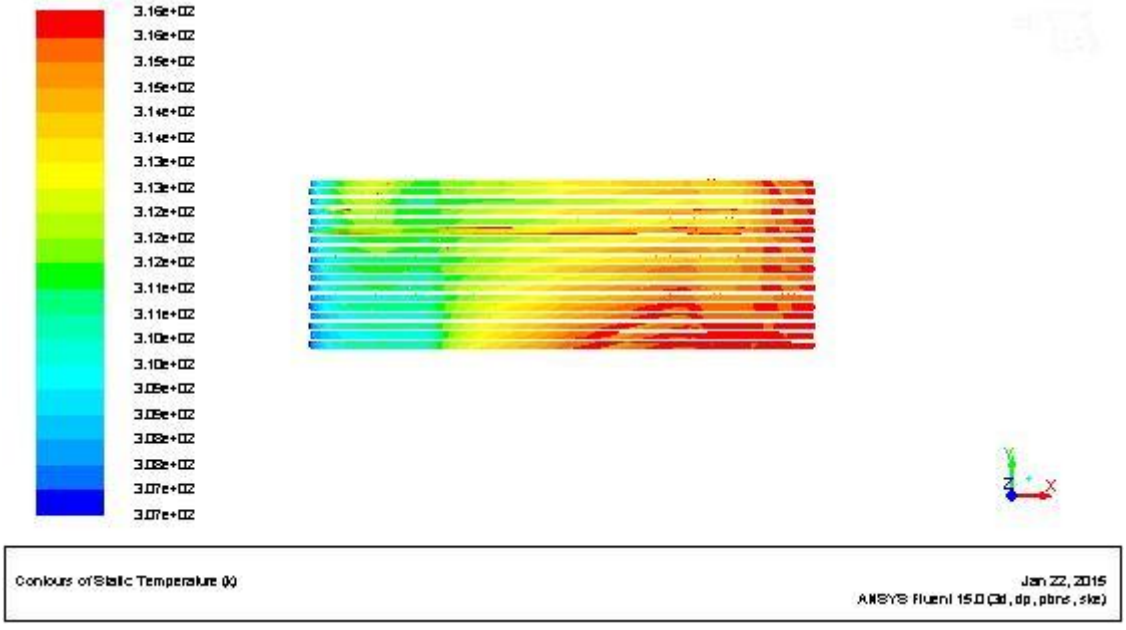

Fig. 4.13: Temperature distribution of cold air

In the fourth section, the temperature drop of hot air is low (12.15 ^{o}C). The reason behind this observation is that the cold air has already gained heat from second section, therefore its capacity to extract further heat from hot air in third section has been reduced. This non uniform temperature distribution pattern of air limits the performance of heat exchanger and in turn the performance of electrical motor.

Velocity distribution of hot air:

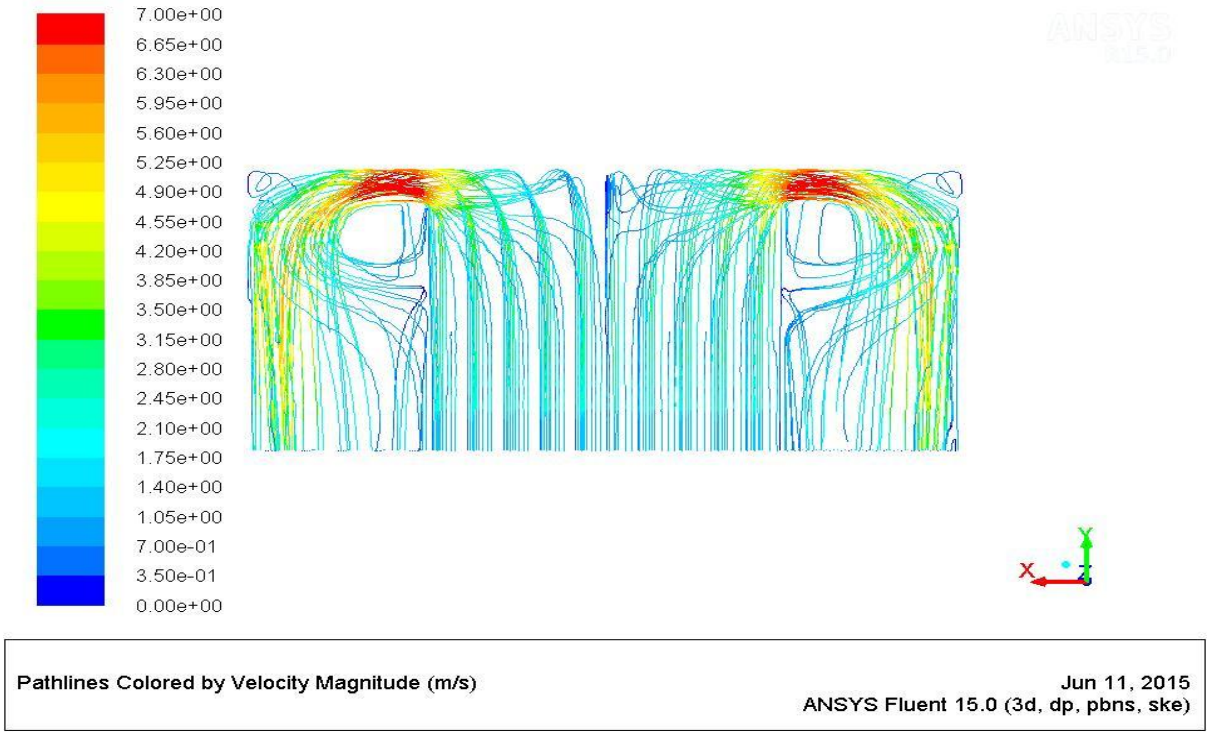

Figure 4.14: Velocity distribution for hot air for actual design

Figure 4.14, shows the velocity distribution of hot air. It can be clearly seen that air is moving upwards at constant velocity and as it crosses the tubes, the velocity of air increases drastically as it moves from one section to another. This increase in the velocity is due to less area for circulation for air at the top of heat exchanger. Hot fluid recirculation has been observed at the top corner of 1st and 4th section. There is some vacant area near the baffles where no air has passed. This is due to high momentum of air which causes air to move outwards. As air passes further through the section some of the air moves towards the vacant

area near the baffle, this is because there is low pressure in the vacant region which pulls the air towards it.

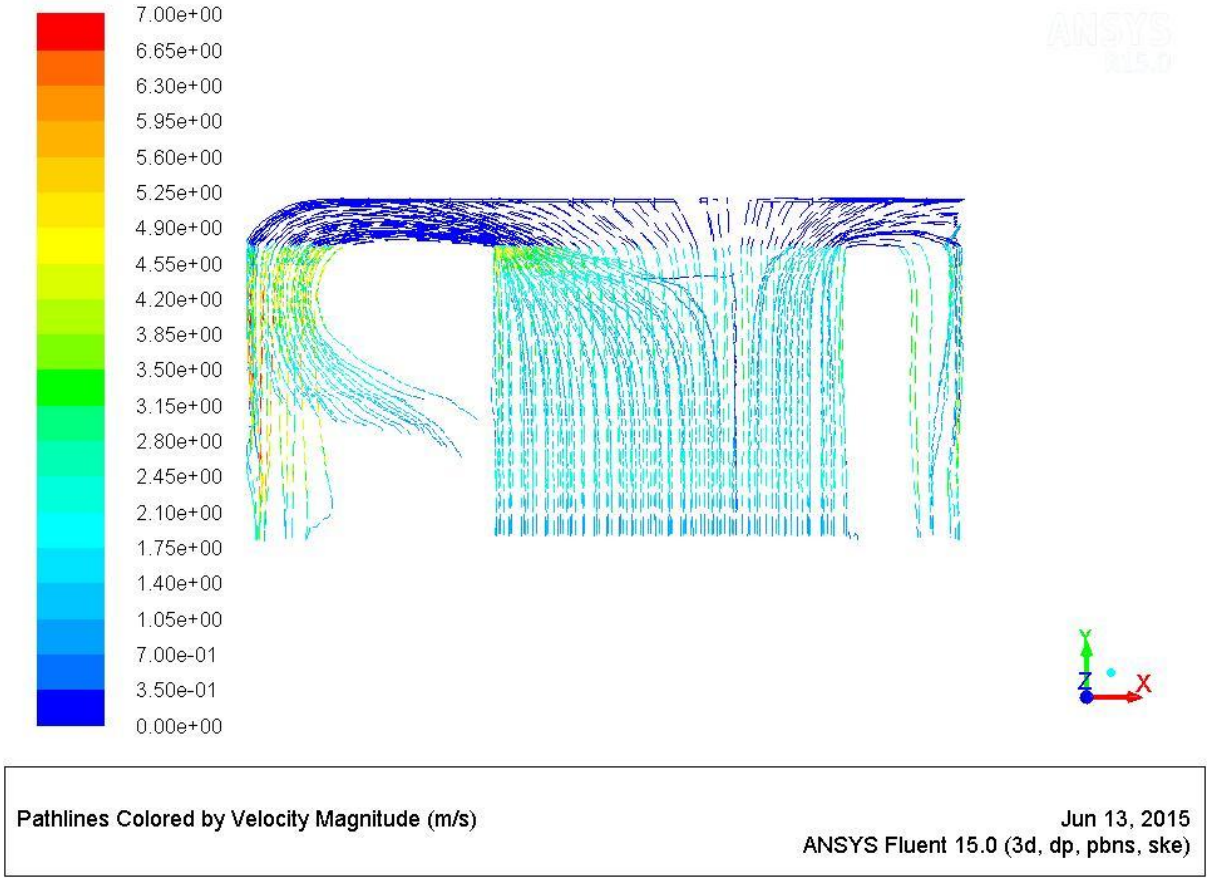

Figure 4.15 : Velocity distribution of hot air for baffle position change model

Figure 4.15, shows the velocity distribution of hot air for change in baffle position. It has been seen that because of change in baffle position more air has remained stagnant in the top portion of the heat exchanger. It can be observed that air is taking turn near the outer baffles which causes more area to be vacant near the vicinity of the internal baffles. This causes improper utilization of area of heat exchanger.

4.4 Comparison of actual and final design

From the results of velocity variation on actual model it has been found that with increase in the velocity there is not much drop in the temperature where as the pressure drop has increased drastically. Also by comparing the different designs it is observed that the addition of three tubes increases the area of heat transfer which leads to increase in heat transfer rate. Hence both of these effects are combined to obtain the final model which was operated at 14 m/s inlet cold air velocity with three additional tubes and the results obtained are compared with the actual model.

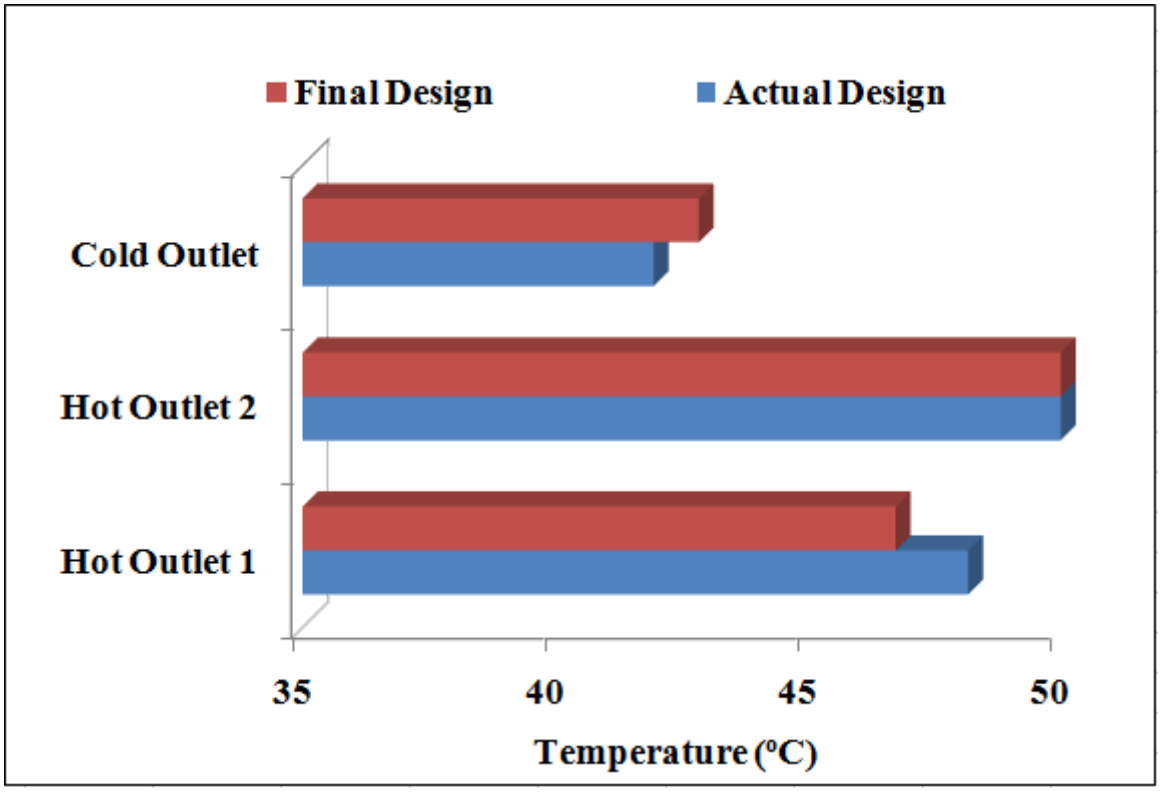

Figure 4.16: Comparison of outlet temperatures between actual and final design

Figure 4.16, shows the comparison of outlet temperatures of cold and hot air of actual design with the final design. It can be seen from the graph that the temperature of the hot outlet 1 has decreased when compared to the actual model whereas the temperature of hot outlet 2 is almost same for both the actual as well as final design. The temperature of the cold air outlet

has increased for final design in comparison to the actual design because of more amount of area and time available for heat transfer.

Figure 4.17, shows the comparison of pressure drop between actual and final design for hot air. It can be seen from the graph that there is slight increase in pressure drop of hot air at both the inlets in final design as compared to actual model. This is because of increase in number of cold air tubes from 27 to30 which causes hindrance in flow of hot air which further leads to increase pressure drop.

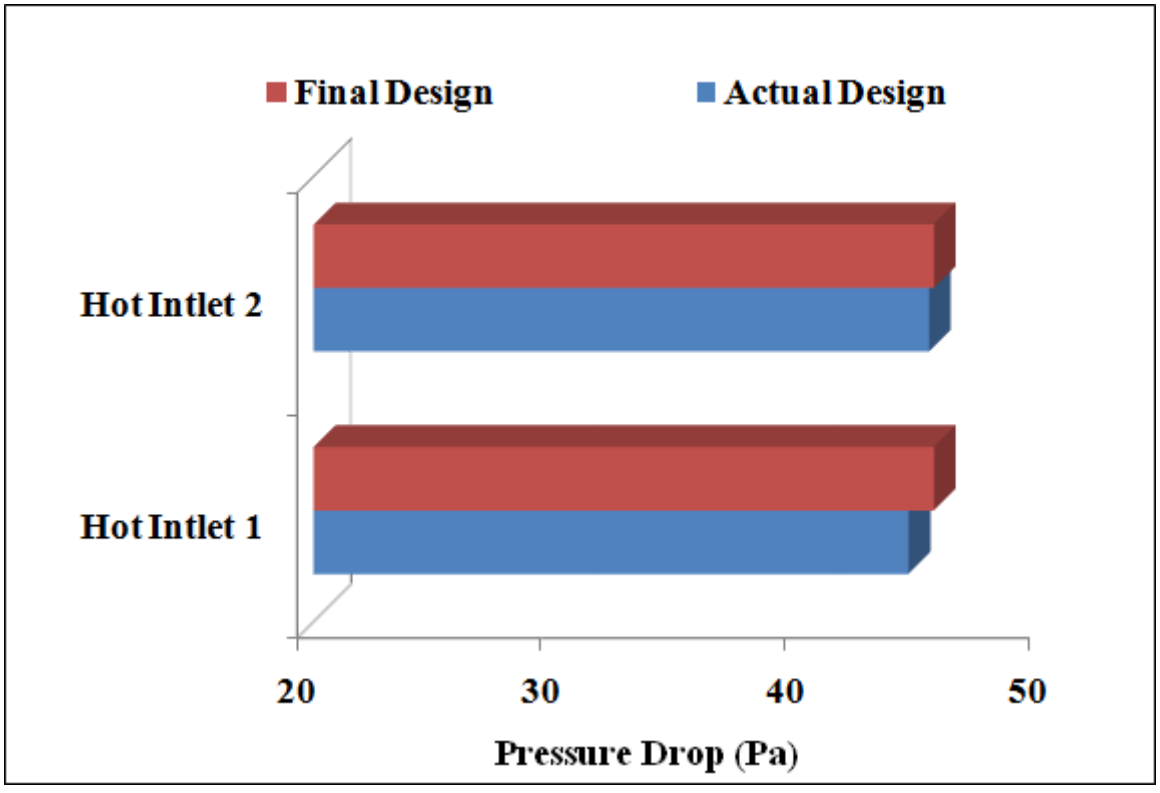

Figure 4.17: Comparison of pressure drop between actual and final design for hot air

Figure 4.18, shows the pressure drop of actual and final design for cold air. It can be seen that there is huge decrease in pressure drop in final design as compared to actual design. The reason for drop in pressure is due increase in number of cold air tubes from 27 to 30 and also due to decrease in cold air velocity from 18 m/s to 14 m/s. The increase in number of cold air

tubes decreases the mass flow rate of cold air passing per tube in the final design when compared with the actual design. The decrease in mass flow rate also decreases the velocity of the cold air passing through the tube. Hence, both the changes directly results in drop in pressure. There is some increase in the pressure in the final design due to increase in number of tubes but its effect was overcome by effect of decrease in velocity as pressure drop is directly proportional to square of velocity (from Darcy Equation).

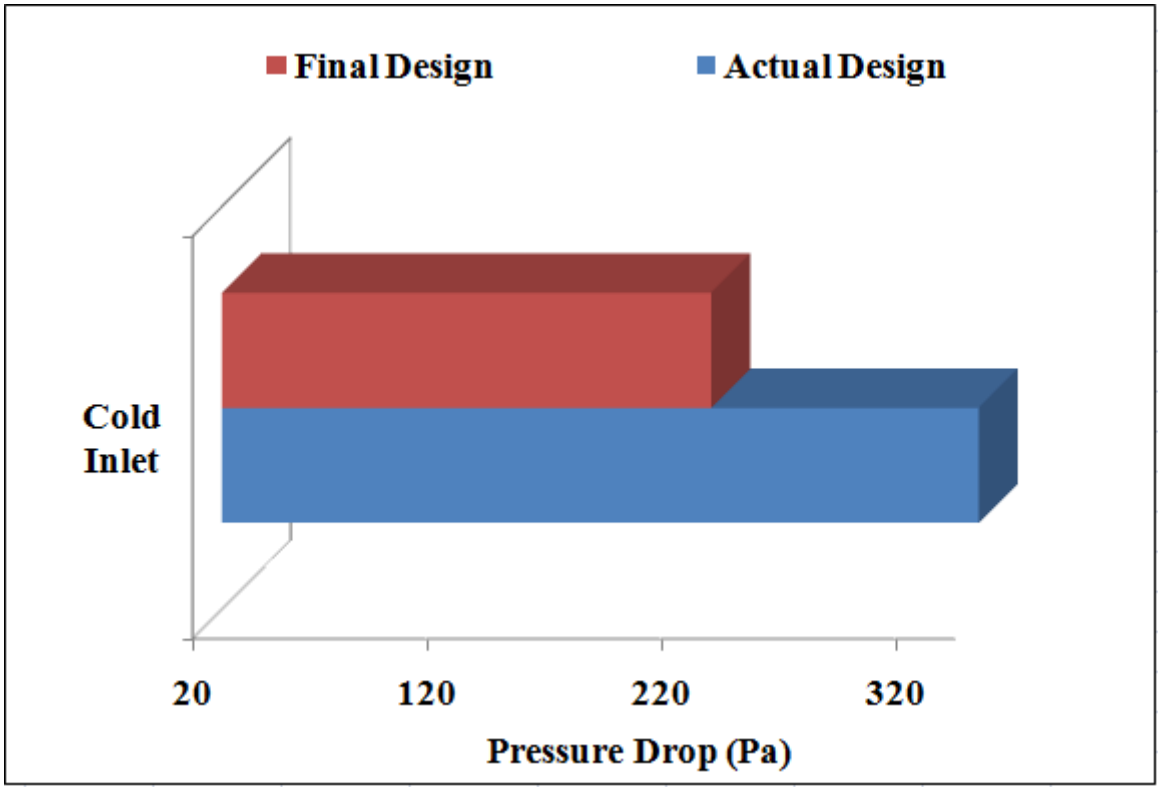

Figure 4.18: Comparison of pressure drop between actual and final design for cold air

With the final proposed design, more effective cooling of hot air was done with 13.52% lesser amount of cold air. Although, there is slight increase in pressure drop of hot air but the decrease in pressure drop of cold air is much significant. So, the effective cooling of the motor could be done at lower pumping power, which in turn decreases the operational cost.

4.5 Comparison of CFD and MATLAB results

Computer Program was developed based on the analytical formation using MATLAB programming for actual design. Geometrical and flow parameters at inlet are supplied as input to the program and the values of thermo-physical parameters of heat exchanger are obtained as output from the program.

Figure 4.19, shows the comparison of outlet temperature between CFD and MATLAB results between hot outlet 1, hot outlet 2 and cold outlet.

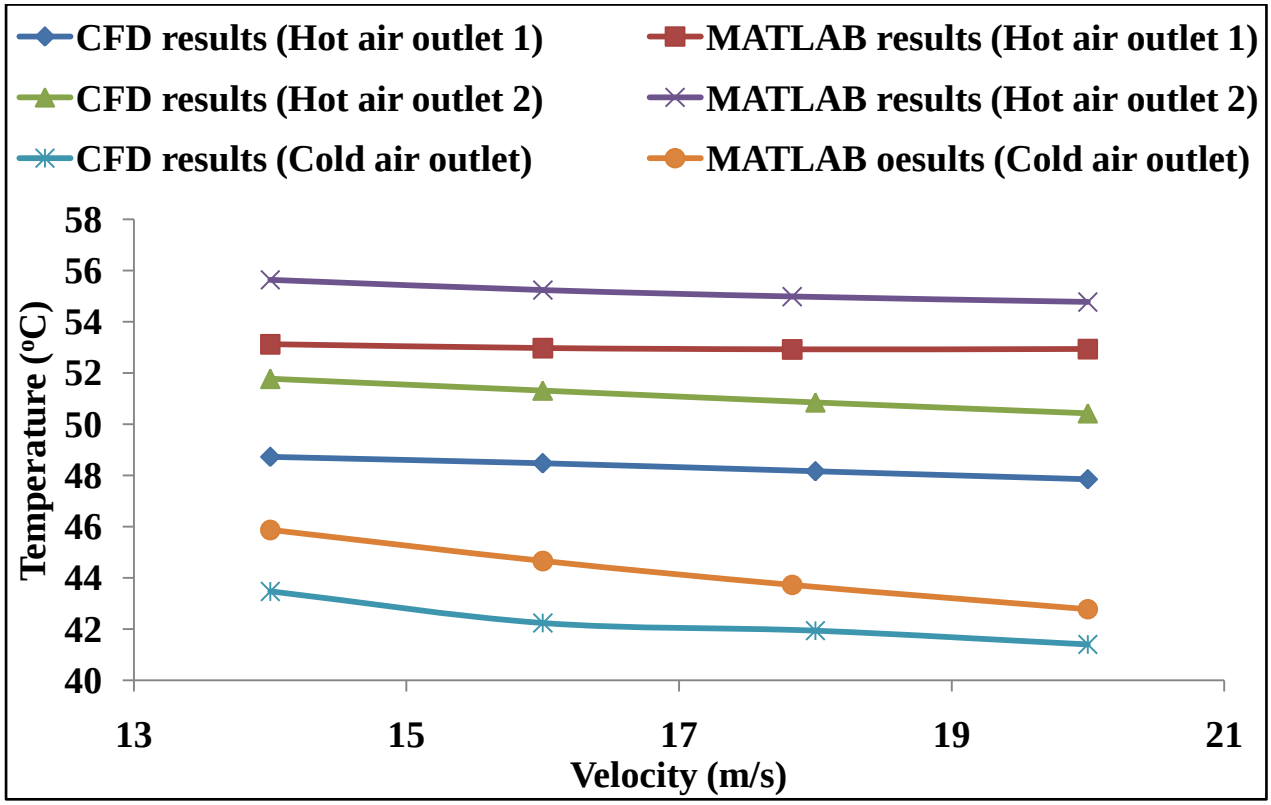

Figure 4.19: Comparison of outlet temperatures between CFD and MATLAB results

Results shown by CFD and MATLAB are in close context with each other for cold air outlet. A maximum error of 5.2% was observed for cold air outlet in between CFD and MATLAB results. An error of 9% has been seen in the results of CFD and MATLAB for hot outlet 1

and hot outlet 2, this is due to neglecting of convective heat transfer coefficient at the top of heat exchanger during MATLAB programming.

Figure 4.20, shows the comparison of pressure drop between CFD and MATLAB results for cold air. Both CFD and MATLAB results shows the same trend i.e. with increase in velocity of air pressure drop inside the tube increases.

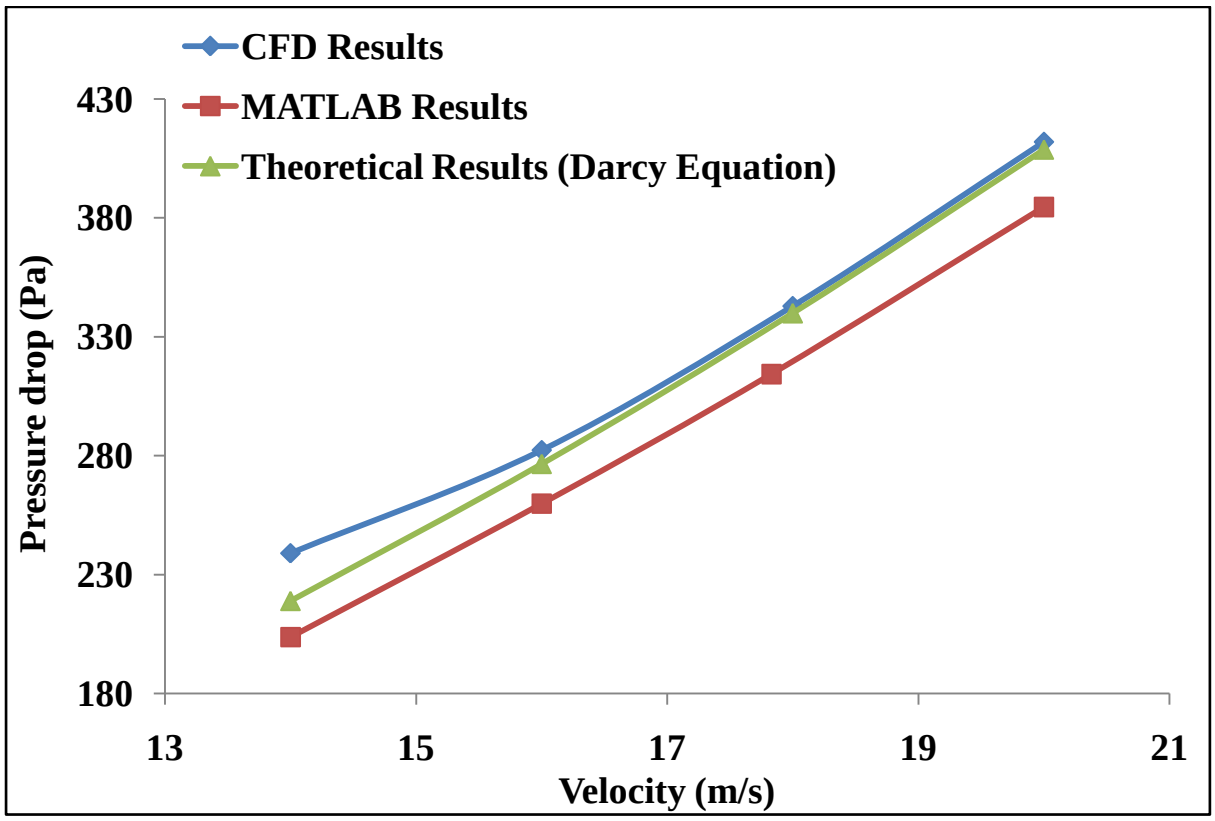

Figure 4.20: Comparison of pressure drop between CFD and MATLAB results

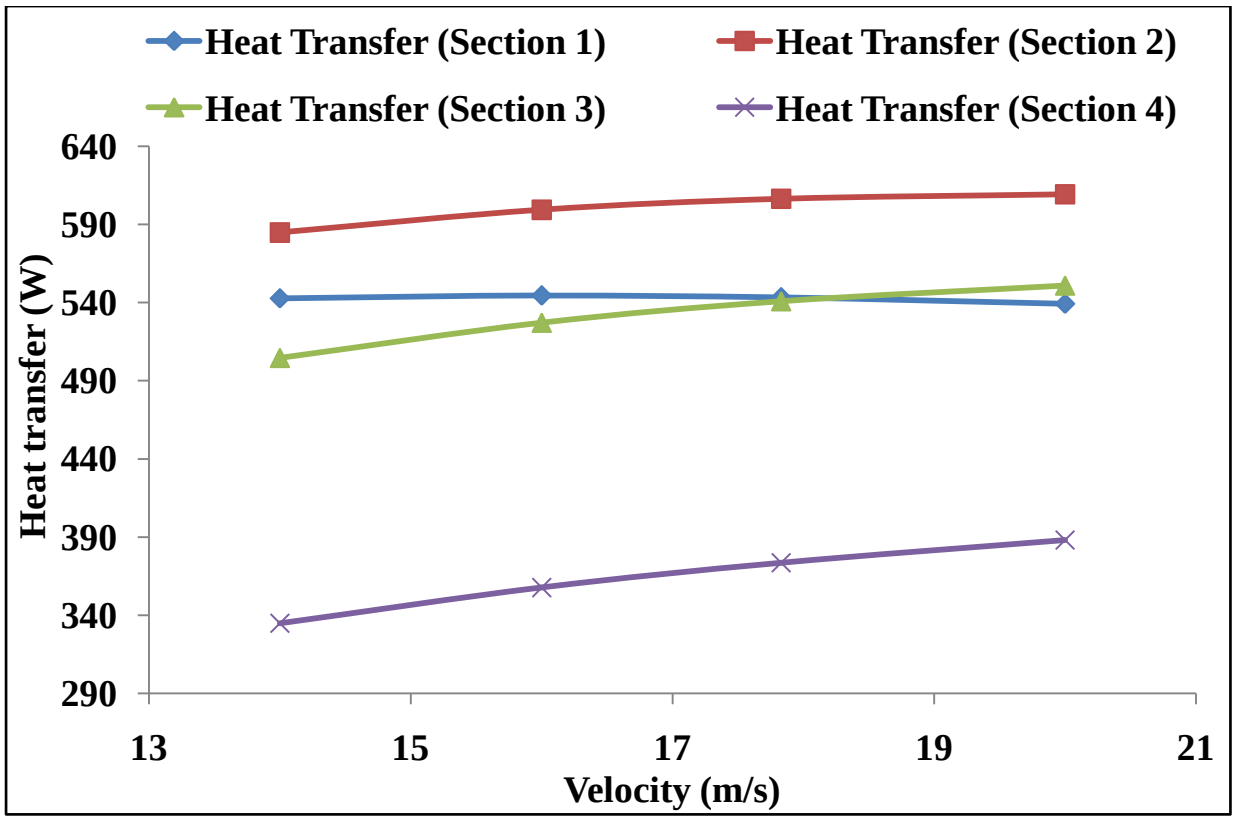

Figure 4.21: Comparison of heat transfer between different sections

Figure 4.21, shows the comparison of heat transfer between the four sections of the heat exchanger. It can clearly seen from the graph that the maximum heat transfer is occurring in section 2 of the heat exchanger. This is because of the fact that in section 2, inlet of hot air takes place, hence there is maximum temperature difference between hot and the cold fluid. Although, section 3 was also the inlet for the hot air but heat transfer in section 3 is less as compared to section 2. This is because the temperature of the cold air has increased while it reaches the third section, hence the temperature difference between the hot and the cold air is less as compared to second section and so is the heat transfer. Heat transfer in case of section 1 and section 3 is almost same. Section 4, shows the least heat transfer because the cold air has almost reached its maximum temperature and the temperature difference between the hot and cold air is very less and hence very less heat transfer.

CHAPTER 5: CONCLUSIONS

The CFD simulation of the air to air tubular cross flow heat exchanger has been performed and following conclusions were made.

- It is found that with increase in velocity of cold air, the temperatures of the hot air decreases due to increase in the heat transfer coefficient.
- The maximum decrease of 4.78% has been obtained in outlet temperature, whereas an increase of 72.39% is observed in pressure drop, when velocity was increased from 14 m/s to 20 m/s. So, 14 m/s cold air inlet velocity was found optimum for operation of heat exchanger.
- Results obtained from MATLAB program has shown close agreement with the CFD simulation results for different cold air inlet velocities.
- It is found the change in location of baffles does not affect much to the outlet temperatures of hot and cold air. .
- The addition of three more tubes has resulted in decrease of outlet temperatures of hot air as well as in pressure drop cold air without having much effect on hot air pressure drop. This is due to increase in area and time available for heat transfer.
- From the velocity distribution, it has been seen that hot air moves from one section to another section of heat exchanger, due to which some area of heat exchanger faces starvation of air near the vicinity of internal baffles. This vacant region is maximum in case of baffle change design.
- It has been observed from the temperature distribution that heat transfer is more effective in the first half of the heat exchanger in comparison to the second half. This is due to the availability of more cold air in first half, because cold air gains some heat

before it enters to the second half. Hence, the temperature of hot air at outlet 2 is always more as compared to temperature of hot air outlet 1.

- A final design three additional tubes and cold air velocity of 14 m/s was found to give better results than actual design with even lesser cold air pressure drop. A decrease of 2.98% is observed in temperature at hot outlet 1 and decrease of 33.29% in cold air pressure drop with proposed design in comparison to actual design.

FUTURE SCOPE OF WORK

The use of air to air tubular cross flow heat exchanger is a growing technology and there are many areas in which further work can be carried out:

(1) Modification in other geometrical parameters such as longitudinal and transverse pitch, diameter of tubes can be varied to further improve the design.

(2) Additional baffles or arrangements can be used to make the flow distribution uniform in first and fourth section of heat exchanger.

(3) Analytical techniques can also be employed to investigate pressure and temperature distribution.

REFERENCE

Andersson, B., Andersson, R., Hakansson, L., Mortensen, M., Studiyo, R. and Wachem, B. V. (2012). *Computational Fluid Dynamics for Engineers.* Publ. Cambridge University Press. 1st Ed.

Aquaro, D. and Pieve, M. (2007). *High Temperature Heat Exchangers for Power plants: Performance of Advanced Metallic Recuperators.* Applied Thermal Engineering. 27: 389-400.

Brandt, H. (1934). *Pressure Drop and Heat Transfer in Tube Heat Exchanger.* Dissertation Hannover Polytechnic.

Buckinx, G, Rogiers, F. and Baelmans, M. (2013). Thermal *Design and Optimization of Small Scale High Effectiveness Cross-Flow Heat Exchangers.* Heat and Mass Transfer. 60: 210-220.

Chilton, T. H., and Generaux, R. P. (1933). *Pressure Drop across Tube Bank*. America Institute Chemical Engg. 29: 161-173.

Chumpia, A. and Hooman, K. (2014). *Performance Evaluation of Single Tubular Aluminium Foam Heat Exchangers.* Applied Thermal Engineering. 66: 266-273.

Chang, C. C., Kuo, Y.F., Wang, J. C. and Chen, S. L. (2010). Air *Cooling for Large Scale Motors.* Applied Thermal Engineering. 30: 1360-1368.

Dixit, T. and Ghosh, I. (2013). *Two Stream Cross Flow Heat Exchangers in Thermal Communication with the Surroundings – A Generalized Analysis.* Heat and Mass Transfer. 66: 1-9.

Du, X.P., Zeng, M., Dong, Z.Y. and Wang, Q.W. (2014). *Experimental Study of the Effect of Air Inlet Angle on the Air-Side Performance for Cross-Flow Finned Oval-Tube Heat Exchangers.* Experimental Thermal and Fluid Science. 52: 146-155.

Farsane, K., Desevaux, P. and Panday, P. K. (2000). *Experimental Study of Cooling of Closed Type Electric Motor.* Applied Thermal Engineering. 20: 1321-1334.

Gangacharyulu, D., Sharma, R. K., Dora, K. B. and Kumar, A. (2004). *Thermal Performance Evaluation of Closed Air Circuit Aircooled (CACA) Heat Exchangers for HighRated Electrical Motors- A case study.* International Journal of Heat Exchangers. International Journal of Heat Transfer. 5: 221-238.

Gnielinski, V. (1976). *New International chemical Engineering*. 16: 359-368.

Gomez, L. C., Navarro, H. A., Godoy, S. M., Campo, A. and Saiz-Jabardo, J. M. (2009). *Thermal Characterization of a Cross-Flow Heat Exchanger with a New Flow Arrangement.* Thermal Sciences. 48: 2165-2170.

Holman, J.P. (1996). *Heat Transfer.* Publ. McGraw-Hill. 8th Ed.

Incropera, F.P. and Dewitt, D.P. (2002). *Fundamentals of Heat and Mass Transfer*. Publ. John Wiley & Sons. 5th Ed.

Ishak, M., Tahseen, A. and Rahman, M.M. (2013). *Experimental Investigations on Heat Transfer and Pressure Drop Characteristics of Air Flow over a Staggered Flat Tube Bank in Cross Flow*. Automotive and Mechanical Engineering. 7: 900-911.

Kast, W. (1974). Pressure *Drop in cross flow across Tube Bundles*. VDI- warmeattas, Section Ld, 2nd edn.

Kumar, V., Gangacharyulu, D., Rao, M.S., and Barve, R.S. (2003-2004). *CFD Analysis of Cross Flow Air to Air Tube Type Heat Exchanger*. Phoneics Journal of Computational Fluid Dynamics and its Applications. 16-17 UK.

Navarro, H. A. and Gomez, L. C. (2005). *A New Approach for Thermal Performance Calculation of Cross Flow Heat Exchangers.* Heat and Mass Transfer. 48: 3880-3888.

Petukhov, B. S., Harnett, J. P., and Irvine T. F. (1970*). Heat Transfer and friction in turbulent pipe flow with variable physical properties, advance in Heat Transfer*. Academic, New York. 6: 1970.

Petukhov, B. S., and Popov, V. M. (1963*). Theoretical calculation of Heat Recovery and frictional resistance in turbulent flow in tubes of an incompressible fluid with variable physical properties, High Temperature*. 1: 69-83.

Pongsoi, P., Pikulkajorn,S., Wang, C.C. and Wongwises, C. (2012). *Effect of Number of Tube Rows on the Air-Side Performance of Crimped Spiral Fin-and-Tube Heat Exchanger with a Multipass Parallel and Counter Cross-Flow Configuration.* Heat and Mass Transfer. 55: 1403-1411.

Sano, Y., Kuwahara, F., Mobedi, M. and Nakayama, A. (2012). *Effects of Thermal Dispertion on Heat Transfer in Cross Flow Tubular Heat Exchangers.* Heat and Mass Transfer. 48: 183-189.

Sieder, E. N. and Tate, G. E. (1936). *Heat Transfer and Pressure Drop of liquids in tubes.* Ind. Engg. Chem. 28:1429.

Staton, D. and Cavagnino, A. (2008). *Convection Heat Transfer and Flow Calculations suitable for Electric Machines Thermal Models.* IEEE Transactions on Industrial Electronics. 55(10): 3509-3516.

Toolthaisong, S. and Kasayapanand, N. (2013). *Effect of Attack Angles on Air Side Thermal and Pressure Drop of the Cross Flow Heat Exchangers with Staggered Tube Arrangement.* Energy Procedia. 34: 417-429.

Versteeg, H. K., and Malalasekera, W. (1995). *An Introduction to Computational Fluid Dynamics*. Publ. Longman Scientific and Technical. 1st Ed.

Webb, R. L. (1971). *A critical evaluation of analytical solutions and Reynolds analogy equations for Heat and Mass Transfer in smooth tubes*. 4: 197-204.

Zukauskas, A. (1968). *Heat Transfer in banks of tubes in cross flow of fluid Thermophysics1*. Academy of Science of the Lithuanian SSR Inst. Of physical and Technical problems of enerrgies, Mintiritnius.

Appendix: A1

Table A1.1: CFD simulation results (temperature and pressures)

Velocity (m/s)	Temperature (^{o}C)			Pressure (Pa)		
	Cold outlet	Hot outlet 1	Hot outlet 2	Cold inlet	Hot inlet 1	Hot inlet 2
14	43.47992	48.73804	51.77844	238.9795	44.39334	45.2314
16	42.24738	48.4747	51.31119	282.3258	44.39334	45.23142
18	41.9433	48.1651	50.85605	342.9379	44.39335	45.23142
20	41.40912	47.85962	50.43283	411.9749	44.39337	45.23141

Table A1.2: MATLAB results (temperature and pressures)

Velocity (m/s)	Temperature (^{o}C)			Pressure (Pa)
	Hot outlet 1	Hot outlet 2	Cold outlet	Cold inlet
14	53.12	55.64	45.87	203.73
16	52.97	55.24	44.66	259.83
17.83	52.92	54.98	43.73	314.29
20	52.93	54.77	42.78	384.58

Table A1.3: MATLAB results (heat transfer through different sections)

Velocity (m/s)	Heat transfer (W)				
	Section 1	Section 2	Section 3	Section 4	Total
14	542.78	584.88	504.64	334.84	1967.1
16	544.53	599.4	527.18	357.69	2028.8
17.83	543.27	606.45	540.86	373.61	2064.2
20	539.31	609.4	551.01	388.1	2087.8

Table A1.4: Comparison of different designs

Model	Hot fluid temperature (^oC)				Cold fluid temperature (^oC)		Pressure drop (Pa)		
	Inlet 1	Outlet 1	Inlet 2	Outlet 2	Inlet	Outlet	Hot inlet 1	Hot inlet 2	Cold fluid
Actual design	63	48.16	63	50.86	34.4	41.94	44.39	45.23	342.93
Baffle position change	63	46.34	63	51.23	34.3	42.05	57.14	28.98	340.83
3 Additional tubes	63	45.72	63	49.51	34.40	42.13	47.43	46.43	340.09

Appendix: A2

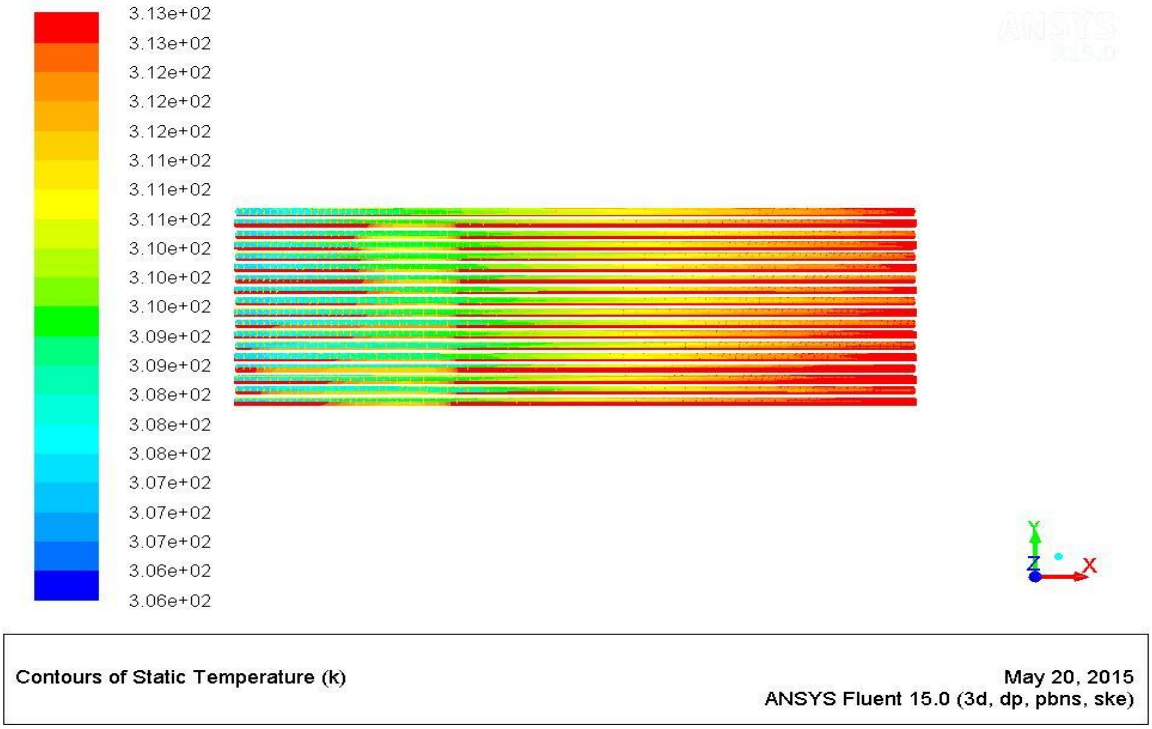

Figure A2.1: Cold air temperature distribution for baffle position change design

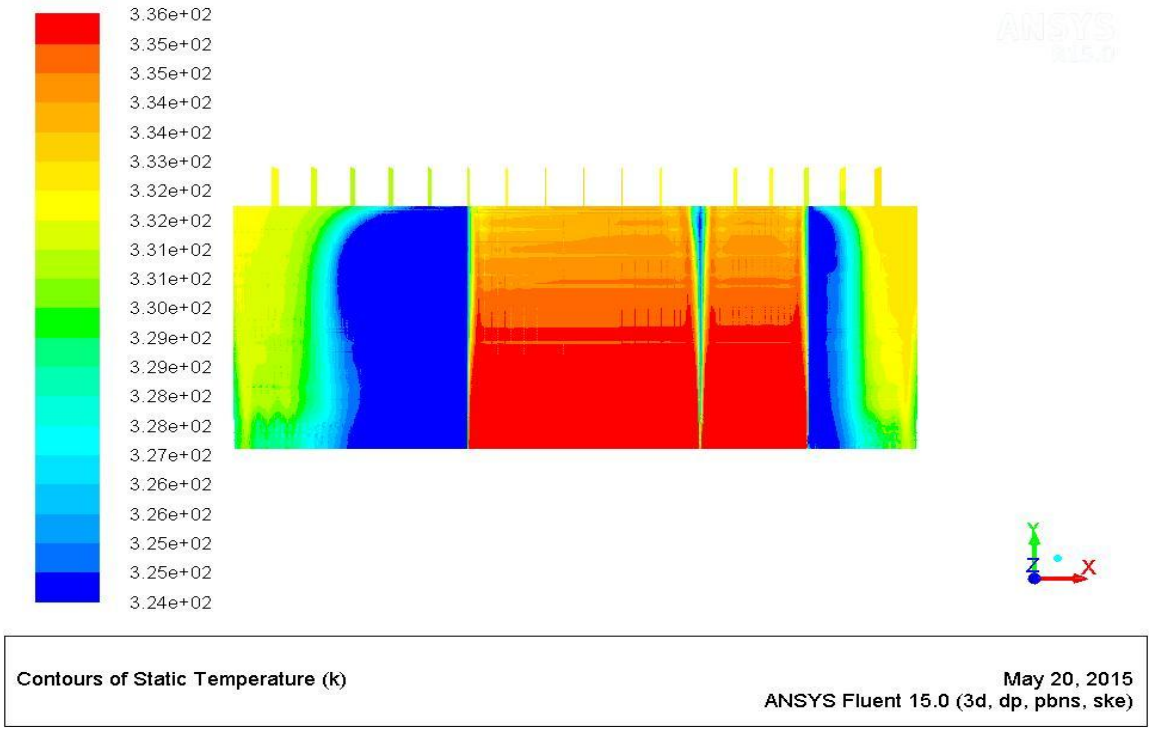

Figure A2.2: Hot air temperature distribution for baffle position change design

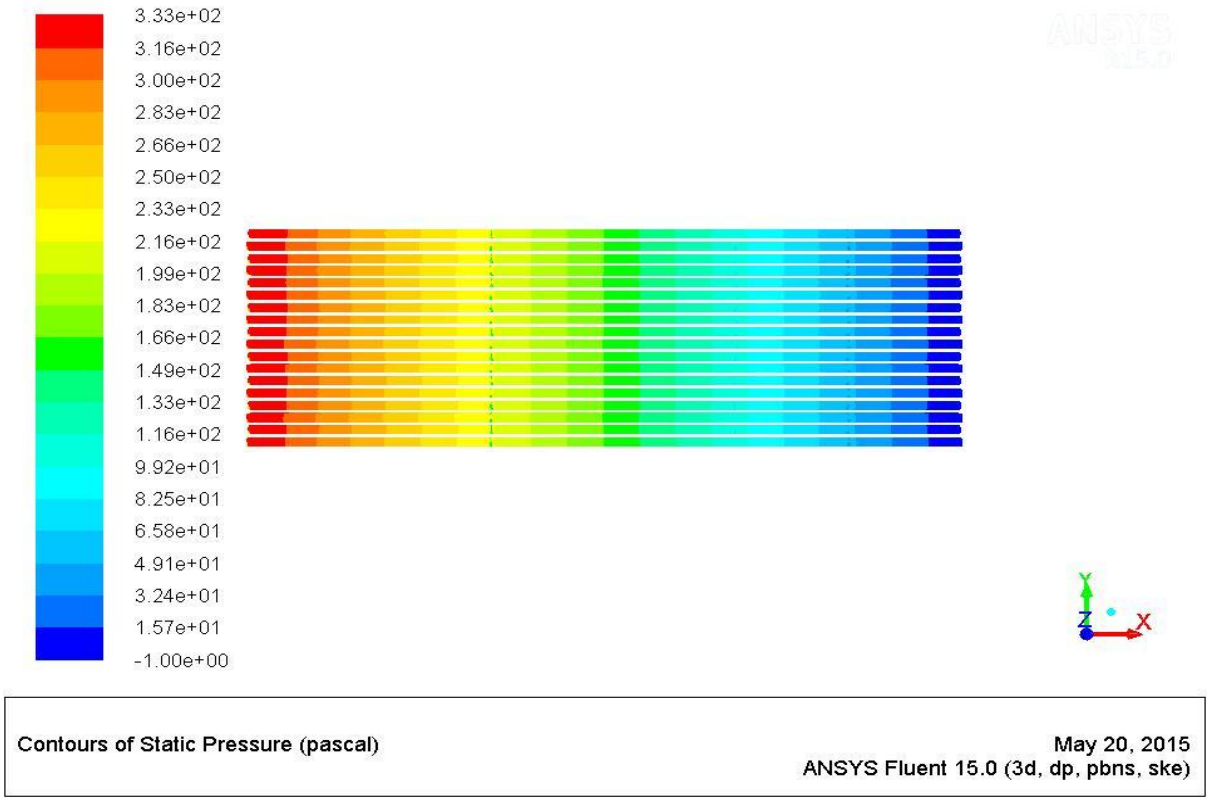

Figure A2.3: Cold air pressure distribution for baffle position change design

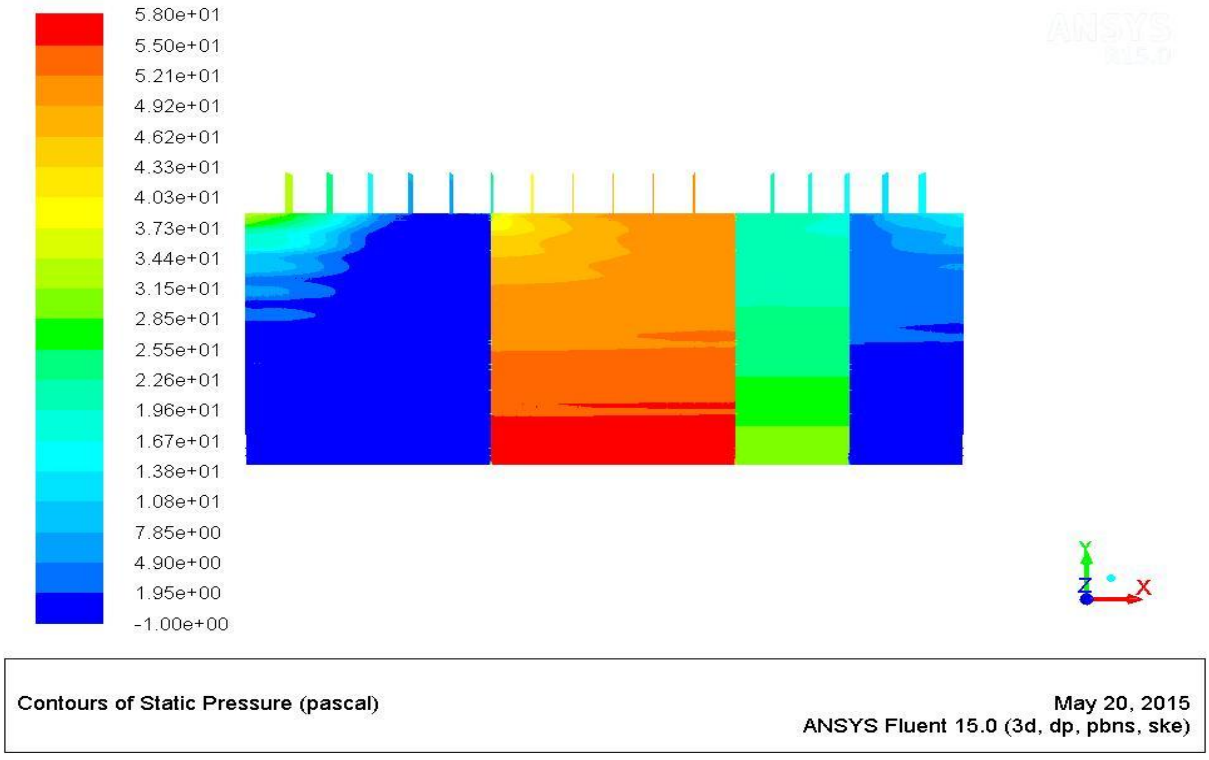

Figure A2.4: Hot air pressure distribution for baffle position change design

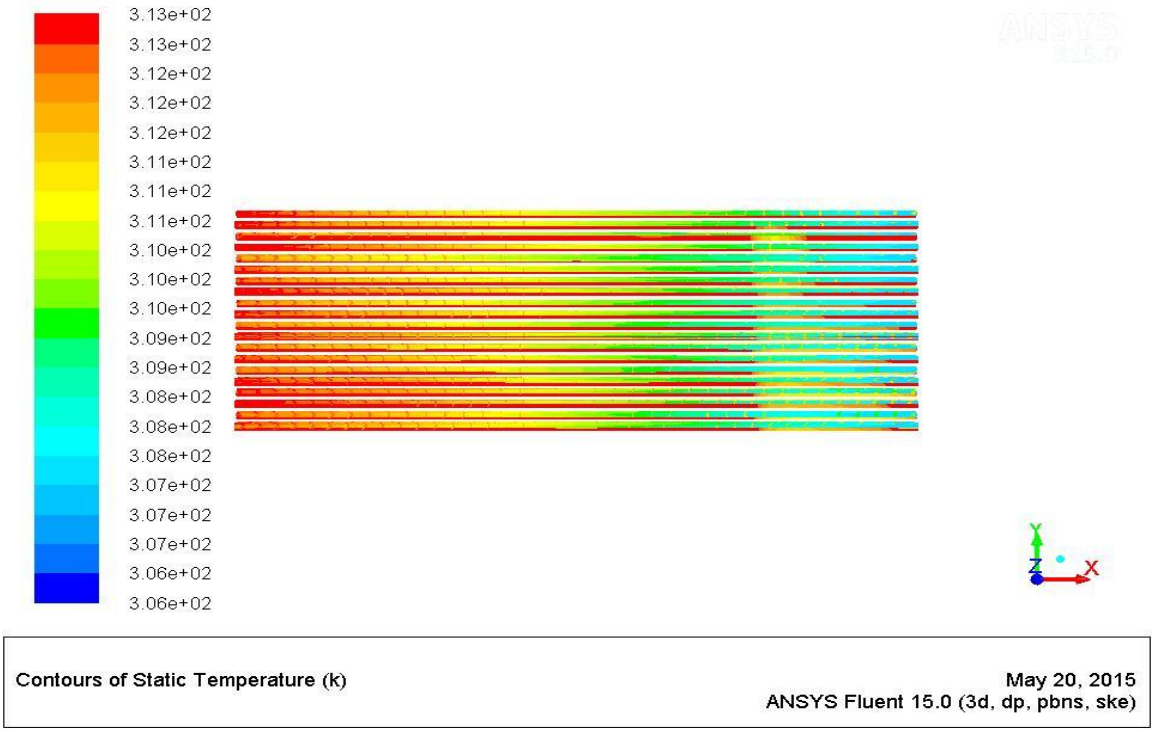

Figure A2.5: Cold air temperature distribution for 3 additional tubes design

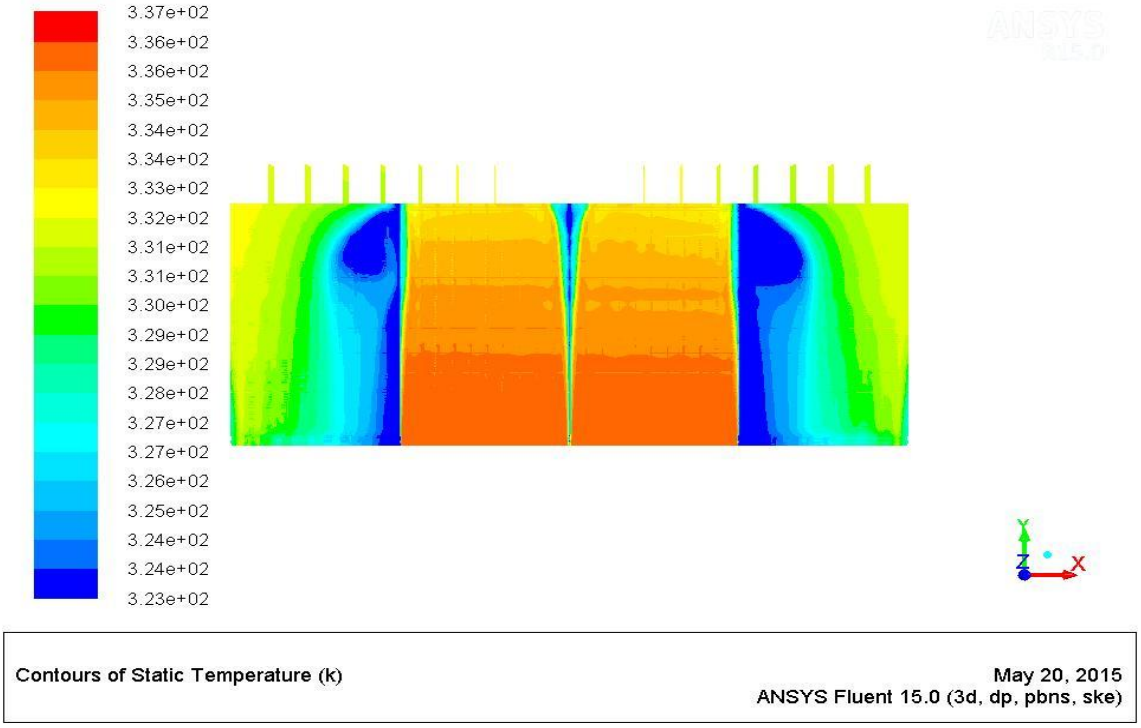

Figure A2.6: Hot air temperature distribution for 3 additional tubes design

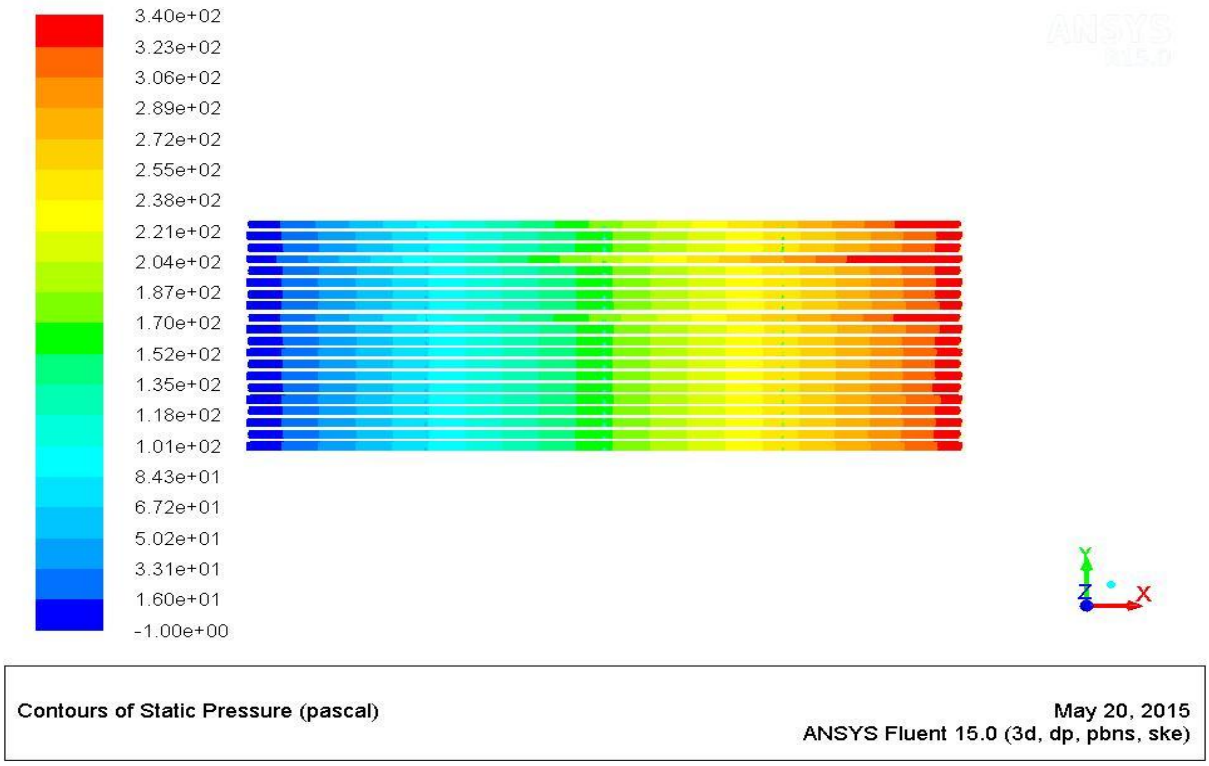

Figure A2.7: Cold air pressure distribution for 3 additional tubes design

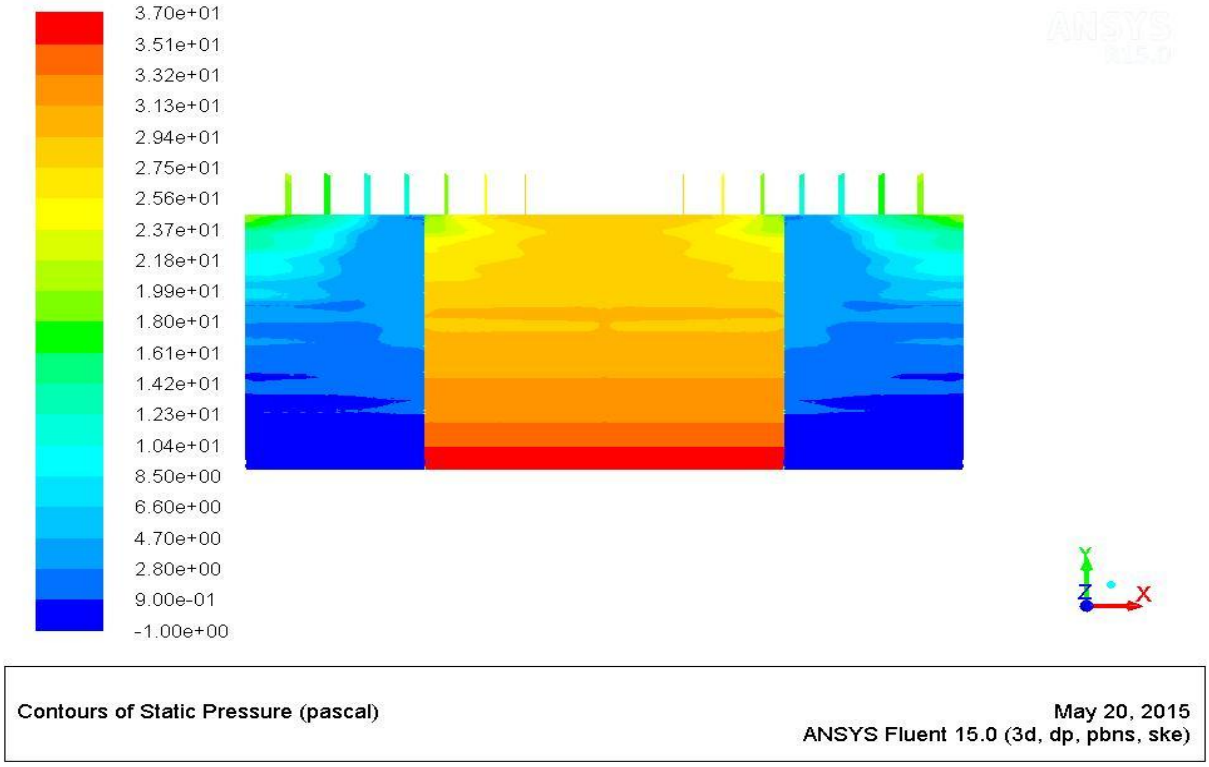

Figure A2.8: Hot air pressure distribution for 3 additional tubes design

Appendix: A3

```
clc;
clear all;
do=0.026;                          %Outer diameter of tubes%
t=0.002;                           %Thickness of tubes%
di=do-2*t;                         %Internal diameter of tubes%
km=54;                             %Thermal conductivity of tube material%
Vh=0.108;                          %Volumetric flow rate of hot air%
Vc=0.183;                          %Volumetric flow rate of cold air%
l=1.61;                            %Length of heat exchanger%
l1=0.39825;                        %Length of heat exchanger section 1%
l2=0.39825;                        %Length of heat exchanger section 2%
l3=l2;                             %Length of heat exchanger section 3%
l4=l3;                             %Length of heat exchanger section 4%
b=0.1;                             %Width of heat exchanger%
Ea=.7;                             %Assumed effectiveness%
Tc1=307;                           %Inlet temperature of cold air%
Th1=336;                           %Inlet temperature of hot air%
rhoc=2.2538-3.588*Tc1*10^(-3);      %Density of cold air at inlet conditions%
rhoh=2.2538-3.588*Th1*10^(-3);      %Density of hot air at inlet conditions%
cpc=985.9+6.6*Tc1*10^(-2);         %Specific heat of cold air at inlet conditions%
cph=985.9+6.6*Th1*10^(-2);         %Specific heat of hot air at inlet conditions%
mc=Vc*rhoc;                        %Mass flow rate of cold air%
mh=Vh*rhoh;                        %Mass flow rate of hot air%
Cc=mc*cpc;                         %Heat capacity rate of cold air%
```

```
Ch=mh*cph;                              %Heat capacity rate of hot air%
T = lakshheat(Ea, Tc1, Th1, Ch, Cc);    %Function call statement%
T1=lakshheat1(T,Ea, Tc1, Th1, Ch, Cc);  %Function call statement%
Tc2=T(1,1);                             %Temperature of cold air at section 1 outlet%
Tc3=T(2,1);                             %Temperature of cold air at section 2 outlet%
Th2=T(3,1);                             %Temperature of hot air at section 2 outlet%
Th3=T(4,1);                             %Temperature of hot air at section 1 outlet%
Tc4=T1(1,1);                            %Temperature of cold air at section 3 outlet%
Th4=T1(1,2);                            %Temperature of hot air at section 3 outlet%
Tc5=T1(1,3);                            %Temperature of cold air at section 4 outlet%
Th5=T1(1,4);                            %Temperature of cold air at section 4 outlet%
Tmh=(Th1+Th3+Th5)/3;                    %Bulk mean temperature of hot air%
Tmc=(Tc1+Tc2+Tc3+Tc4+Tc5)/5;            %Bulk mean temp of cold air%
[rho,meu,cp,k,Pr] = propertyfunc (Tmc); %Property function call statement%
vi=Vc/(3.14*27*0.011^2);                %Velocity of cold air at tube inlet%
Re=rho*vi*di/meu;                       %Reynolds number for inner side of tube%
f=0.316/Re^0.25;                        %Friction factor for tube%
Pi=rho*f*l*vi^2/(2*di);                 %Pressure drop for tube%
Nui=.023*(Re^.8)*(Pr^.4);               %Nusselt number at inner side of tube%
hi=Nui*k/di;                            %Heat transfer coefficient at inner side of tube%
Cc=mc*cp;                               %Heat capacity rate of cold air%
[rho,meu,cp,k,Pr] = propertyfunc (Tmh); %Property function call statement%
vo=Vh/(2*l1*b);                         %Velocity of hot air%
vmax=vo*0.0205/(sqrt((0.0205^2)+(0.0305^2))-do);
                                        %Maximum velocity of hot air across tube bundles%
```

```
Red=rho*vmax*do/meu;                    %Reynolds number across tube bundle%
Nuo=0.4*Red^0.6*Pr^0.36;                %Nusselt number across tube bundle%
ho=Nuo*k/do;                            %Heat transfer coefficient across tube bundle%
Ch=mh*cp;                               %Heat capacity rate of hot air%
U=1/((1/hi)+(3.14*di*di*log(do/di))/(4*2*3.14*l1*km)+(di/(ho*do)));
                                        %Overall heat transfer coefficient%
As=3.14*di*l1*27;                       %Area of heat transfer per section%
NTU=U*As/Ch;                            %Number of transfer units%
C=Cc/Ch;                                %Heat capacity ratios%
Ec=1-exp((exp(-NTU*C*NTU^-0.22)-1)/(C*NTU^-0.22));
                                        %Calculated effectiveness%
e=abs(Ea-Ec);                   %Error between assumed and calculated effectiveness%
while (e>0.01)                          %While loop condition%
Tc1=307;
Th1=336;
rhoc=2.2538-3.588*Tc1*10^(-3);
rhoh=2.2538-3.588*Th1*10^(-3);
cpc=985.9+6.6*Tc1*10^(-2);
cph=985.9+6.6*Th1*10^(-2);
mc=Vc*rhoc;
mh=Vh*rhoh;
Cc=mc*cpc;
Ch=mh*cph;
T = lakshheat(Ea, Tc1, Th1, Ch, Cc);
T1=lakshheat1(T,Ea, Tc1, Th1, Ch, Cc);
```

```
Tc2=T(1,1);

Tc3=T(2,1);

Th2=T(3,1);

Th3=T(4,1);

Tc4=T1(1,1);

Th4=T1(1,2);

Tc5=T1(1,3);

Th5=T1(1,4);

Tmh=(Th1+Th3+Th5)/3;

Tmc=(Tc1+Tc2+Tc3+Tc4+Tc5)/5;

[rho,meu,cp,k,Pr] = propertyfunc (Tmc);

vi=Vc/(3.14*27*0.011^2);

Re=rho*vi*di/meu;

f=0.316/Re^0.25;

Pi=rho*f*l*vi^2/(2*di);

Nui=.023*(Re^.8)*(Pr^.4);

hi=Nui*k/di;

Cc=mc*cp;

[rho,meu,cp,k,Pr] = propertyfunc (Tmh);

vmax=vo*0.0205/(sqrt((0.0205^2)+(0.0305^2))-do);

Red=rho*vmax*do/meu;

Nuo=0.4*Red^0.6*Pr^0.36;

ho=Nuo*k/do;

Ch=mh*cp;

U=1/((1/hi)+(3.14*di*di*log(do/di))/(4*2*3.14*l1*km)+(di/(ho*do)));
```

```
As=3.14*di*l1*27;
NTU=U*As/Ch;
C=Cc/Ch;
Q1=Ch*(Th2-Th3);                    %Heat transfer through section 1%
Q2=Ch*(Th1-Th2);                    %Heat transfer through section 2%
Q3=Ch*(Th1-Th4);                    %Heat transfer through section 3%
Q4=Ch*(Th4-Th5);                    %Heat transfer through section 4%
Q=Q1+Q2+Q3+Q4;                      %Total heat transfer rate%
Ec=1-exp((exp(-NTU*C*NTU^-0.22)-1)/(C*NTU^-0.22));
e=abs(Ea-Ec);
Ea=(Ea+Ec)/2;                       %Assumed effectiveness for next iteration%
end

%Property function%

function [ rho, meu, cp, k, Pr ] = propertyfunc( T )
rho=2.2538-3.588*T*10^(-3);
meu=4.734*10^(-8)+4.576*10^(-8)*T;
cp=985.9+6.6*T*10^(-2);
k=(3.5*10^(-3))+(7.58*T*10^(-5));
Pr=(0.774)+(-2.2*T*10^(-4));
end

%Function to calculate temperatures at section 1 and 2%
```

```
function [ T ] = lakshheat(Ea, Tc1, Th1, Ch, Cc)
if Ch>Cc
    A=[-1 0 Ea 0;
    (1-Ea) -1 0 0;
    -Cc 0 Ch -Ch;
    Cc -Cc -Ch 0];
B=[(Ea-1)*Tc1;
    -Ea*Th1;
    -Cc*Tc1;
    -Ch*Th1];
    T=linsolve(A,B);
else
    A=[0 0 (Ea-1) 1;
    -Ea 0 1 0;
    -Cc 0 Ch -Ch;
    Cc -Cc -Ch 0];
B=[Ea*Tc1;
    (1-Ea)*Th1;
    -Cc*Tc1;
    -Ch*Th1];
    T=linsolve(A,B);
end
end
```

%Function to calculate temperatures at section 3 and 4%

```
function [ T1 ] = lakshheat1( T, Ea, Tc1, Th1, Ch, Cc )
Tc2=T(1,1);
Tc3=T(2,1);
Th2=T(3,1);
Th3=T(4,1);
if Ch>Cc
    Tc4=((1-Ea)*Tc3)+Ea*Th1;
    Th4=Th1-((Cc/Ch)*(Tc4-Tc3));
    Tc5=((1-Ea)*Tc4)+(Ea*Th4);
    Th5=Th4-((Cc/Ch)*(Tc5-Tc4));
else
    Th4=(1-Ea)*Th1+Ea*Tc3;
    Tc4=Tc3+(Ch/Cc)*(Th1-Th4);
    Th5=((1-Ea)*Th4)+(Ea*Tc4);
    Tc5=Tc4+(Ch/Cc)*(Th4-Th5);
end
T1=[Tc4 Th4 Tc5 Th5];
end
```

PUBLICATIONS

Lakshya Garg, Sumeet Sharma, D. Gangacharyulu. Numerical Analysis of Tubular Cross Flow Heat Exchanger using CFD. Published in proceeding of "Paradigms shift in Management and Technology" (PSIMT 2015) April 09-10-2015 at YMCA University of Science and Technology Faridabad.

Lakshya Garg, Sumeet Sharma, D. Gangacharyulu,. Parametric Analysis of Air to Air Tubular Cross Flow Heat Exchanger using Computational Fluid Dynamics. **Experimental Thermal Fluid Science, Elsevier.** (Communicated)